


Spring 5-2023

Molecular Evidence for the Export of Terrigenous Organic Matter to the North Gulf of Mexico by Solid-State ^{13}C NMR and Fourier Transform Ion Cyclotron Resonance Mass Spectrometry of Humic Acids

Sarah Ann Ware
Old Dominion University, ceraann1@gmail.com

Follow this and additional works at: https://digitalcommons.odu.edu/chemistry_etds

 Part of the [Analytical Chemistry Commons](#), [Biogeochemistry Commons](#), and the [Environmental Sciences Commons](#)

Recommended Citation

Ware, Sarah A.. "Molecular Evidence for the Export of Terrigenous Organic Matter to the North Gulf of Mexico by Solid-State ^{13}C NMR and Fourier Transform Ion Cyclotron Resonance Mass Spectrometry of Humic Acids" (2023). Master of Science (MS), Thesis, Chemistry & Biochemistry, Old Dominion University, DOI: 10.25777/a8xa-q953
https://digitalcommons.odu.edu/chemistry_etds/71

This Thesis is brought to you for free and open access by the Chemistry & Biochemistry at ODU Digital Commons. It has been accepted for inclusion in Chemistry & Biochemistry Theses & Dissertations by an authorized administrator of ODU Digital Commons. For more information, please contact digitalcommons@odu.edu.

**MOLECULAR EVIDENCE FOR THE EXPORT OF TERRIGENOUS ORGANIC
MATTER TO THE NORTH GULF OF MEXICO BY SOLID-STATE ^{13}C NMR AND
FOURIER TRANSFORM ION CYCLOTRON RESONANCE MASS SPECTROMETRY
OF HUMIC ACIDS**

by

Sarah Ann Ware
B.S. May 2015, Old Dominion University

A Thesis Submitted to the Faculty of
Old Dominion University in Partial Fulfillment of the
Requirements for the Degree of

MASTER OF SCIENCE

CHEMISTRY

OLD DOMINION UNIVERSITY
May 2023

Approved by:

Patrick G. Hatcher (Director)

Hongmei Chen (Member)

Kenneth Mopper (Member)

Balasubramanian Ramjee (Member)

ABSTRACT

MOLECULAR EVIDENCE FOR THE EXPORT OF TERRIGENOUS ORGANIC MATTER TO THE NORTH GULF OF MEXICO BY SOLID-STATE ^{13}C NMR AND FOURIER TRANSFORM ION CYCLOTRON RESONANCE MASS SPECTROMETRY OF HUMIC ACIDS

Sarah Ann Ware
Old Dominion University, 2023
Director: Patrick G. Hatcher

Marine organic matter is mainly believed to originate from autochthonous organic matter, while terrigenous organic matter is assumed to be largely degraded prior to reaching the open ocean or more recently replaced by marine organic matter via a stripping process. Sediment samples along a transect extending from the Mississippi River Birdsfoot Delta to the Mississippi Canyon on the Louisiana continental shelf were examined by advanced analytical techniques, electrospray ionization coupled to a 12T Fourier transform ion cyclotron resonance mass spectrometer (ESI-FTICR-MS) and quantitative solid-state multiple cross polarization magic angle spinning (multi-CPMAS) ^{13}C NMR in an effort to understand the source and export of terrigenous organic matter to the Gulf of Mexico. Both NMR and mass spectral data indicate that condensed aromatics (CA) and carboxyl-containing aliphatic molecules (CCAM) are present at the mouth of the river, we suggest a high contribution from terrigenous soil-like organic matter. With seaward progression, CA mass spectral peak magnitudes diminish by 15% and, correspondingly, 30% of integrated NMR peak areas. In contrast, mass spectral and NMR CCAM peaks grow by 7 and 13% respectively. These trends suggest that data collected from this investigation using humic acid extracts shows molecular evidence of terrigenous organic matter deposited in offshore sediments.

This thesis is dedicated to my husband, Aaron Berman, without whom I would not have finished my bachelor's degree let alone dreamt of going to graduate school. I love you more than words can say.

ACKNOWLEDGEMENTS

First and foremost I would like to express my sincere thanks to my advisor, Dr. Patrick Hatcher, for his support and guidance throughout my graduate studies. Dr. Hatcher has listened to my failings, my concerns, my victories and everything in between with an understanding ear and extremely helpful advice. I would like to thank my group members past and present for their support, encouragement, and margarita outings; Dr. Derrick Waggoner, Dr. Hongmei Chen, Stephanie Hagberg (née McElheine), Macey Cohen, Dr. Alex Goronov, Dr. Rachel Sleighter, Scarlet Aguilar-Martinez, Nathan Jentik, Samantha Sullivan, Hannah Hammontree, Louis Bondurant and honorary member Morgan Daniels. Many people at Old Dominion University have helped me along my journey and deserve thanks for all they have done towards my gathering of knowledge and reprieve from the stresses of graduate life. Those people include but not limited to faculty, staff and students alike. The Frank Batten Endowment Fund, and the National Science Foundation [CHE-1610021] deserve my gratitude for funding my research, and a special thanks to Tammy Subotich, for her wit, smile, and safe haven.

For the people that are most important in my life, I would like to thank my family and friends for their love and support and especially for enduring the explanations of my research. To my parents and my children for their unconditional love and optimism, I will always cherish your encouragement. To my husband, without whom I literally could not have accomplished any of this, you pushed me to be better, you listened to my wild ideas and even contributed to them, then you helped me walk through more than a few.

NOMENCLATURE

%C	Percent Carbon
%N	Percent Nitrogen
^{13}C	Carbon 13 isotope
^1H	Hydrogen 1 isotope
Ad/Al	Acid/Aldehyde ratio
C	Carbon
C/N	Carbon/Nitrogen ratio
C3	Plant that uses 3-Carbon acid for carbon dioxide fixation
C4	Plant that uses 4-Carbon acid for carbon dioxide fixation
CA	Condensed aromatics
CCAM	Carboxyl-containing aliphatic molecules
CHN	Carbon, hydrogen, nitrogen containing molecules
CHO	Carbon, hydrogen, oxygen containing molecules
CHON	Carbon, hydrogen, oxygen, nitrogen containing molecules
CHOS	Carbon, hydrogen, oxygen, sulfur containing molecules
COO	Carbon, dioxide functional groups within molecules

CuO	Copper oxide
$\delta^{13}\text{C}$	Delta carbon 13
DOM	Dissolved organic matter
ESI-FTICR-MS	Electrospray ionization coupled to Fourier transform ion cyclotron resonance mass spectrometry
H/C	Hydrogen/carbon ratio
HA	Humic acid
HMW	High molecular weight
KMD	Kendrick mass defect
$\Lambda 8$	Lambda 8, total weight in milligrams of the sum of the vanillyl, syringyl and cinnamyl phenols normalized to 100 mg of organic carbon
LMW	Low molecular weight
multi-CPMAS	Multiple cross polarization magic angle spinning
N	Nitrogen
NMR	Nuclear magnetic resonance
O	Oxygen
O/C	Oxygen/carbon ratio
OC	Organic carbon
OM	Organic matter

PAH	Polycyclic aromatic hydrocarbons
POM	Particulate organic matter
terrOM	Terrigenous organic matter
vK	van Krevelen

TABLE OF CONTENTS

	Page
LIST OF FIGURES	ix
Chapter 1	1
1. INTRODUCTION	1
2. EXPERIMENTAL METHODS	6
SAMPLES AND INITIAL PROCESSING	6
HUMIC ACID EXTRACTION	7
ELEMENTAL ANALYSIS	8
SOLID-STATE ¹³ C NMR SPECTROMETRY	8
ULTRAHIGH RESOLUTION MASS SPECTROMETRY	9
3. RESULTS	11
HUMIC ACID EXTRACT YIELDS	11
GENERAL CHARACTERISTICS OF SOLID-STATE ¹³ C NMR	11
FTICR-MS DATA	15
4. DISCUSSION	17
NMR	17
ESI-FTICR-MS	21
5. CONCLUSIONS	29
REFERENCES	32
APPENDICES	38
A. FIGURES S1-S8	38
B. TABLE S1	46
VITA	47

LIST OF FIGURES

Figure	Page
1. Bathymetric map showing the locations of sediment transect collected by Sampere et al. (2008) and 8064-whole sediment by Richard Bennett (Hatcher, 1980).	7
2. Solid-state ^{13}C NMR spectra for 3 humic acid extracts from sediment along the transect; River, 80 m, Canyon and a whole sediment sample collected near the mid-point of the transect for comparison, labeled as sample 8064.	12
3. Relative peak intensity percentages (r %) of molecular data for the HA extracts from FTICR-MS analysis (MS) and NMR peak data converted by the structural assignment software proposed by Baldock et al. (2004).	14
4. Negative ion ESI-FTICR-MS data for humic acid extracts at the mouth of the river sample. The van Krevelen plot includes a log scale of relative intensities indicated by the color bar.	22
5. Negative ion ESI-FTICR-MS data for humic acid extracts of the canyon sample. The van Krevelen plot includes a log scale of relative intensities indicated by the color bar.	24
6. (a) K8 values (mg lignin/ 100 mg organic carbon) from CuO oxidation analysis and stable carbon isotopic composition for the whole sediment measured by Sampere et al. (2008), lignin % from FTICR-MS data (summation of peak magnitudes for lignin-like formulae).	25
7. Comparison of the formulae between the river and the canyon.	26

CHAPTER 1

INTRODUCTION

The carbon cycle and therefore the tracking of carbon are integrally important for the carbon models used in many different scientific studies. One such analysis involves terrigenous versus marine organic matter (OM) and the transport of OM through the world's river systems that are eventually deposited into oceans. The origin of coastal sedimentary OM that eventually forms Type II kerogen and associated Type II petroleum in ancient rocks had been considered to be mainly derived from marine autochthonous OM deposited in coastal depocenters. On a global scale, 80% of OM deposited in marine sediments is deposited in these depocenters (Hedges and Oades, 1997b). These include upwelling areas, deltaic accretionary wedges, submarine canyons and downwarping shelf basins (Hedges and Keil, 1995, Smith and Mackenzie, 1987). Terrigenous organic matter (*terrOM*) is proximal to such depocenters in the form of riverine-transported OM (Schlesinger and Melack, 1981) and export from coastal wetlands, as well as back barrier island complexes. Global annual carbon fluxes from major rivers have been shown to be 1.06 Pg, recently updated by Li et al. (2017). Early estimates report that about half of the inland carbon delivered by rivers worldwide is consumed and respired as CO₂ (Berner, 1989, Hedges et al., 1992, Hedges and Keil, 1995, Mayorga et al., 2005), however, these estimates were mostly based on bulk measurements. These studies suggest that this *terrOM* was extensively degraded and lost as CO₂ and H₂O before reaching kerogen-forming depocenters (Hedges and Oades, 1997a, Hedges et al., 1994, Kirchman and Suzuki, 1991, Middelburg et al., 1993, Sugimura and Suzuki, 1988) however, more recent studies have shown this not to be the case (Sampere et al., 2008, Kuliński et al., 2016, Wu et al., 2019). Much of the evidence for degradation in deltaic large-river regions occurs in

mobile-muds, a process that has been referred to as “incineration” of organic matter because of the highly oxidative conditions in these sedimentary deposits (Aller, 1998, Blair and Aller, 2011). Resuspension of sediments through storm events, particularly hurricanes and tropical storms which are prevalent in this region, can also cause extensive oxidation of the sediments to occur (Bianucci et al., 2018, Moriarty et al., 2018). Other pathways for rapid decay of *terrOM* may be linked with photochemical or microbial degradation (Opsahl and Benner, 1998) and algal-primed processing during transport (Bianchi, 2011a). In many cases, stable isotopic and chemical biomarker indices reflect differential decay of different chemical components of *terrOM*, linked in part with hydrodynamic sorting, during transport to offshore sediments (Bianchi et al., 2007, Prahl et al., 1994, Wakeham et al., 2009). More recently, Blattmann et al. (2019) suggest that stripping of *terrOM* from clays followed by replacement with marine carbon can explain the fate of *terrOM*.

In the Mississippi/Atchafalaya River system, the focus of the current study, one observes a classic two-end-member mixing between isotopically depleted terrigenous carbon signals and isotopically enriched marine autochthonous signals. It is well known that the Mississippi/Atchafalaya River system has a large contribution of both C_3 and C_4 plants from the Mississippi River flood basin and coastal marshes. Goñi et al. (1997, 1998) suggest that the overprint of soil from C_4 -dominated grassland plants probably compromises the use of the two-end-member model for estimating allochthonous contributions and that terrigenous carbon contributions to offshore sediments are much greater than predicted by the simple isotope mixing model. Moreover, Goñi et al. (1997, 1998) employed the classical lignin phenol analyses coupled to compound-specific stable carbon isotopic analyses to evaluate possible contribution of C_4 plants from soils. Other work presented by Gordon and Goñi (2003, 2004), using a three-endmember mixing model, show *terrOM* accounts for about 65-80% of the organic matter deposited on the inner shelf of the

Mississippi/Atchafalaya systems supporting Goñi et al. (1997, 1998). Lignin-phenol biomarkers suggested that offshore *terrOM* is more represented by terrestrial components, presumably due to selective removal of the more labile OM algal fractions during transport (Bianchi et al., 2002, Mead and Goñi, 2006). CuO oxidation techniques used for the many lignin phenol calculations can be misleading because the chemical processes that occur do not completely depolymerize the lignin macromolecule which can result in only 1% of OM representation (Hernes et al. 2013, Klotzbücher et al. 2016). Lithogenic-rich fine particles containing lignin derived from aged soil sources are distributed further offshore with much less alteration (Goñi et al., 1998, Gordon and Goñi, 2004, Sampere et al., 2008, Waterson and Canuel, 2008). Finally, another source of *terrOM* in this region is coastal marsh inputs (Bianchi et al, 2011c) from one of the most rapidly eroding coastal zones in the world (Giosan et al., 2014), except for a few prograding sites (Shields et al., 2017). This non-riverine *terrOM* input, largely ignored by earlier studies in their offshore transport models, certainly complicates the role of the C₄ sources because of the similar $\delta^{13}\text{C}$ signatures of distant mid-west grasslands and local marsh sources (Bianchi, 2011c). Other anthropogenic effects, such as significant reductions in the suspended inorganic sediment load due to trapping of mineral particles behind dams (de la Rosa et al., 2011), has also altered the fraction of organic to mineral contents of particles entering the coastal zone from the Mississippi/Atchafalaya River system (Allison et al., 2007). Goñi et al. (1997) also imply that this pattern of fluctuating terrigenous carbon export may be responsible for climate driven isotopic excursions in nearshore depocenters commonly attributed to paleo-productivity variations brought about by sea-level fluctuations.

We report here some advanced molecular-based results that have bearing on the export of soil-derived OM in the Mississippi/Atchafalaya River system to the Gulf of Mexico. This work builds

on the existing literature, however, we employ quantitative multi-CP solid-state ^{13}C NMR technique in combination with electrospray ionization Fourier transform ion cyclotron resonance mass spectrometer (ESI-FTICR-MS) to examine sedimentary OM and humic extracts of OM in this region. Combining NMR and FTICR techniques to analyze DOM is an approach used by Hertkorn et al. (2006), Grinhut et al. (2011) and Hertkorn et al. (2016) to examine deep ocean DOM, wetland DOM and microbially degraded humic acids, respectfully, implementing various liquid state ^1H NMR pulse programs in their analyses. DiDonato et al. (2016) utilized solid state multi-CPMAS ^{13}C techniques to analyze humic acids from soil OM and further characterize the molecules populating the three regions outlined in our van Krevelen plots (CCAM, lignin-like, and condensed aromatics). Here we chose to use the same approach as DiDonato to discern if molecules associated with terrigenous humic acids are present and if they persist onto the continental shelf.

Previously examined sediment samples from a transect extending from the Mississippi river mouth to the head of the Mississippi Canyon that transects the Louisiana continental shelf were used in this study (Sampere et al., 2008). The previous study focused on lignin phenols (markers for terrigenous material), plant pigments (markers for both terrigenous and autochthonous material), and stable isotopic compositions of sediments. Our goal is to combine the data from the current study with markers from the Sampere et al. (2008) study to better understand the origin and export of organic matter across the Mississippi shelf. The use of humic acid extracts was specifically chosen for two distinct reasons; 1) solubility is essential for ESI-FTICR-MS, and 2) fulvic acids, the other component of alkaline extracts, are commonly saturated with salts that interfere with charge competition in the ESI and would require further processing to remove the salts. Using humic acids allowed for less chemical processing thereby limiting the possibility of alterations to

the samples. One could also employ water extraction, but this is less efficient, and salts still present a problem with ESI-FTICR-MS. While humic acids account for only about 10% of sedimentary organic matter, we contend that they could be more representative of the bulk sedimentary organic matter than previously employed biomarkers. We envision that such an approach used in the current study might also be applicable to other deltaic systems worldwide.

CHAPTER 2

EXPERIMENTAL METHODS

SAMPLES AND INITIAL PROCESSING

Sediment samples were collected in July 2003, as described by Sampere et al. (2008). Collection was from the seaward transect extending across the Louisiana Continental Margin from the mouth of the Mississippi River Birdsfoot Delta to the head of the offshore Mississippi Canyon that extends to a distance of 92 km and a water depth of 540 m (Fig. 1, Table 1). A 50 cm² box-corer was used to retrieve the sediment samples. They were frozen while still on-board ship and then freeze-dried at onshore-based laboratories. Freeze-dried sediments were later extracted with deionized water to mainly remove salts. The wet residues were then extracted with a dilute (10%) hydrochloric acid solution to solubilize carbonates and alkali cations from association with organic acids. Following an ultrapure water wash and air-drying, the sediment residues were extracted with a 1:1 methylene chloride: methanol mixture. Following centrifugation and removal of the organic extraction mixture by decantation, fresh solvent mixture was added, and the sonication extraction was repeated at least twice followed by a pure methanol extraction. After subsequent air-drying, the residues were stored in a desiccator prior to humic acid extraction. One of the sediment samples, referred to hereafter as 8064-whole sediment, was collected in 1976 by Richard Bennett, as described by Hatcher (1980), this sample was located in the vicinity of the above-mentioned transect (Fig. 1).

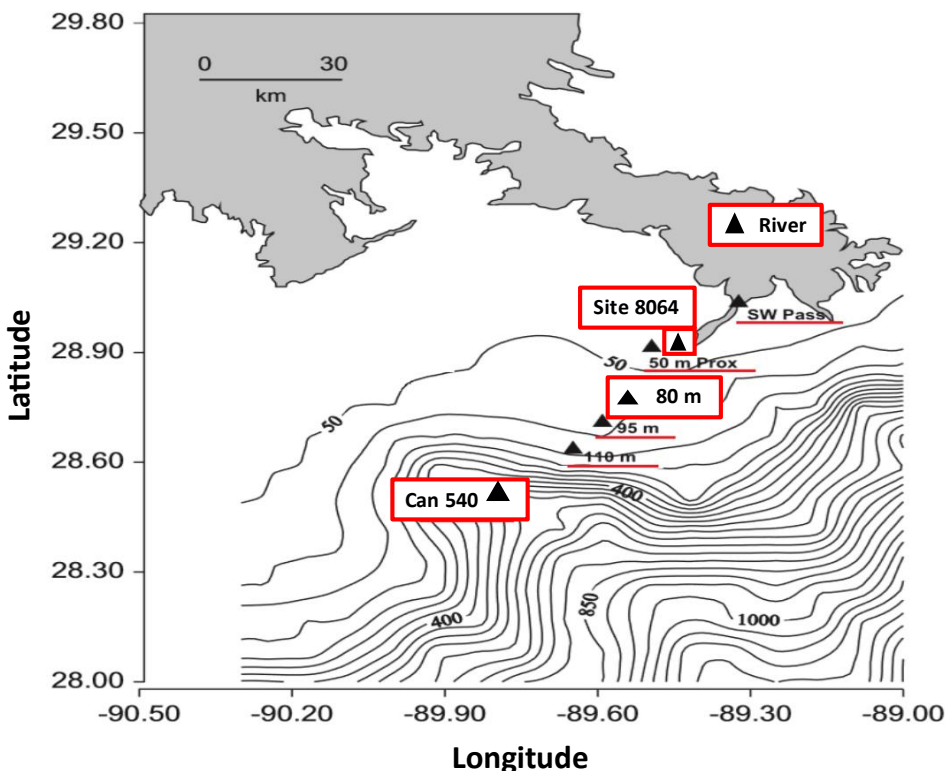


Fig. 1. Bathymetric map showing the locations of sediment transect collected by Sampere et al. (2008) and 8064-whole sediment by Richard Bennett (Hatcher, 1980). Boxed sites represent samples used in solid state ^{13}C NMR. Sample sites are listed by either location or the sediment depth below sea level. Details of each sample is listed in Table 1. Map was modified and used with permission, previously published in Sampere et al. (2008).

HUMIC ACID EXTRACTION

Alkaline extraction of the dried sediment samples was carried out with 0.5 M NaOH under a blanket of nitrogen. The containers were placed in an incubator shaker table at 25°C and 150 rpm overnight. The sediment/alkali mixture was centrifuged, the soluble extract separated from sediment by decantation, washed several times with fresh alkali solution, and centrifuged and decanted again until alkali extracts were colorless. The total supernatant was treated by cation

exchange resin (Dowex AG) for deionization. The eluent, consisting of operationally defined fulvic and humic acids, was acidified to pH 2 resulting in the precipitation of the humic acids. The precipitated humic acids were separated from the fulvic acid fraction by centrifugation and freeze-dried for 24 hours to remove any excess water. Solid-state ^{13}C NMR studies required more sample than was available in most cases, thus, three sediment samples for which sufficient material was available were chosen for analysis, river, 80m, and canyon. Humic acid yields per gram of whole sediment for each sample were 3.75, 4.5, 5.5 mg/g dry weight, respectively.

ELEMENTAL ANALYSIS

Elemental composition for total carbon, hydrogen and nitrogen (CHN) was performed on both the whole sediment sample and humic acid extractions using a CE Elantech Flash EA 1112 series elemental analyzer. Quantification was achieved using a calibration curve of nicotinamide and aspartic acid standards. Samples were prepared, with the same tin cups used for the standards, in triplicate for consistency.

SOLID-STATE ^{13}C NMR SPECTROSCOPY

A 400 MHz Bruker Avance II NMR spectrometer equipped with a 2.5 mm H-X probe was used to analyze the solid humic acid fractions. Quantitative spectra were obtained via a multi-CPMAS pulse program described in Johnson and Schmidt-Rohr (2014) and used by Hartman et al. (2015). Briefly, multi-CPMAS allows direct polarization results to be obtained five times faster due to CP ramp on the ^1H channel consisting of 11 steps of 100 μs duration with a 1% amplitude increment (Johnson and Schmidt-Rohr, 2014). The humic acid samples were packed into a 2.5 mm ceramic

rotor and sealed with a Kel-F cap. The 8064-whole sediment sample was analyzed directly after freeze-drying using the same pulse sequence described above, with a 4 mm zirconium rotor and sealed with a Kel-F cap. Acquisition parameter included a spectral frequency of 100 MHz and 400 MHz for ^{13}C and ^1H , respectively. The 2.5 mm rotor, filled with humic acid, was spun at 15 kHz allowing for the reduction or elimination of spinning side bands and acquired 5k scans in approximately 5 hours. The 4 mm rotor housing the whole sediment was spun at 14 kHz and acquired 64k scans to maximize the signal to noise, for approximately 2 days. Integration of the spectra included parsing out chemical shift regions according to Nelson and Baldock (2005). These chemical shift regions are defined here: aliphatic carbon regions (0-45 ppm for unsubstituted aliphatic carbons, 45-110 ppm for O and N-substituted alkyl carbons), aromatic carbons (110-160 ppm), and double-bonded oxygenated carbons (160-220 ppm for carboxyl, amide, ketone, and aldehyde carbon) and are illustrated in Fig. 2.

ULTRAHIGH RESOLUTION MASS SPECTROMETRY

For ESI-FTICR-MS analysis, a 100 ppm solution was made from the dried solid HA. An aqueous solution of 0.1 M NH_4OH was used to dissolve the solid HA and subsequently diluted 50:1 with methanol/water. The pH 8 aqueous methanol solution was analyzed by a Bruker Daltonics 12T Apex Qe FTICR-MS using an Apollo II negative mode electrospray ionization (ESI), procedures detailed in Sleighter and Hatcher (2008). An external calibration of the instrument was carried out, prior to samples being introduced, with polyethylene glycol standard. Each sample was then optimized for spray shield current as well as ion accumulation times which was determined to be 5.0 s due to poor charging of the HA. During instrumental analysis 300 scans were co-added over a m/z range of 200-1200. Resulting peaks were calibrated using naturally present fatty acids and

other homologous series in the samples (Sleighter and Hatcher, 2008). After removal of peaks from the procedural blank, analyte peaks were assigned unique elemental formulae via an in house Matlab (The MathWorks, Inc. Natick, MA) formula calculator (Obeid, 2015) within 1 ppm error. Elemental data from thousands of these formulae were plotted on van Krevelen diagrams (Kim et al., 2004, Van Krevelen, 1950) to ascertain the chemical characteristics of the formulae observed. Formula verification can be achieved in several ways. One is to confirm major peaks have a corresponding ^{13}C peak, accomplished within our Matlab coding. Another verification method is to determine if molecules fall into a series by way of Kendrick Mass Defect analysis which is also built into our Matlab code and processed in Excel macros. For this purpose, Kendrick Mass Defect (KMD) plots of COO functional group were constructed from the data (supplemental Fig. S2). The COO functional group was chosen because these samples exhibited a large contribution of aromatic and carboxyl signals in the NMR spectra, and secondly humic acids are known to contain structures which are thought to have abundant carboxyl functional groups (Kramer et al., 2004). KMD plots showed a homologous series of formulae where the defect was the exact difference of a COO group (Sleighter and Hatcher, 2007). The formulae that appeared in a series were plotted on a horizontal line and were assumed to be in the same series. This type of analysis and formula assignment is referred to as ‘formula extension’ which allows for better assignment of higher molecular weight mass to charge (m/z) data points, greater than 500 m/z (Sleighter and Hatcher, 2008).

CHAPTER 3

RESULTS

HUMIC ACID EXTRACT YIELDS

Listed in Table 1 are the locations of the transect samples along with elemental carbon and nitrogen contents and ratios, and lambda 8 (Λ_8) values from Sampere et al. (2008) and Waterson and Canuel (2008). Λ_8 is defined as the total weight in milligrams of the sum of the vanillyl, syringyl and cinnamyl phenols normalized to 100 mg of organic carbon (Hedges and Parker, 1976). This table also includes the carbon-normalized contribution of humic acid to the whole sediment carbon content. Humic acid carbons make up approximately 12.6, 14.1, 18.3% of the total organic carbon in the river, 80m, and canyon sediment samples, respectively. The remainder consists of lipids, methanol soluble substances, fulvic acids and insoluble kerogen-like OM.

GENERAL CHARACTERISTICS OF SOLID-STATE ^{13}C NMR

Three of the seven transect samples and a whole sediment sample, collected separately from a site near the transect and previously described by Hatcher (1980) were analyzed using the same multi-CPMAS pulse program. The three transect samples were chosen for their positions in the transect and these samples provided enough solid humic acid required for the 2.5mm rotor. The whole sediment was chosen for comparison because of its proximity to the transect (Fig. 2). NMR spectra for both the transect and 8064 whole sediment show similar chemical shift characteristics with some minor differences in magnitude for peaks in the region of 160-220 ppm and 45-110 ppm.

This similarity suggests that the humic acid fractions are approximately representative of the entire organic matter in these sediments. The whole sediment and associated humic acids are composed mainly of peaks in aliphatic carbon regions (0-45 ppm for unsubstituted aliphatic carbons, 45-110 ppm for O and N-substituted alkyl carbons), aromatic carbons (110-160 ppm), and double-bonded oxygenated carbons (160-220 ppm for carboxyl, amide, ketone, and aldehyde carbon) (Fig. 2).

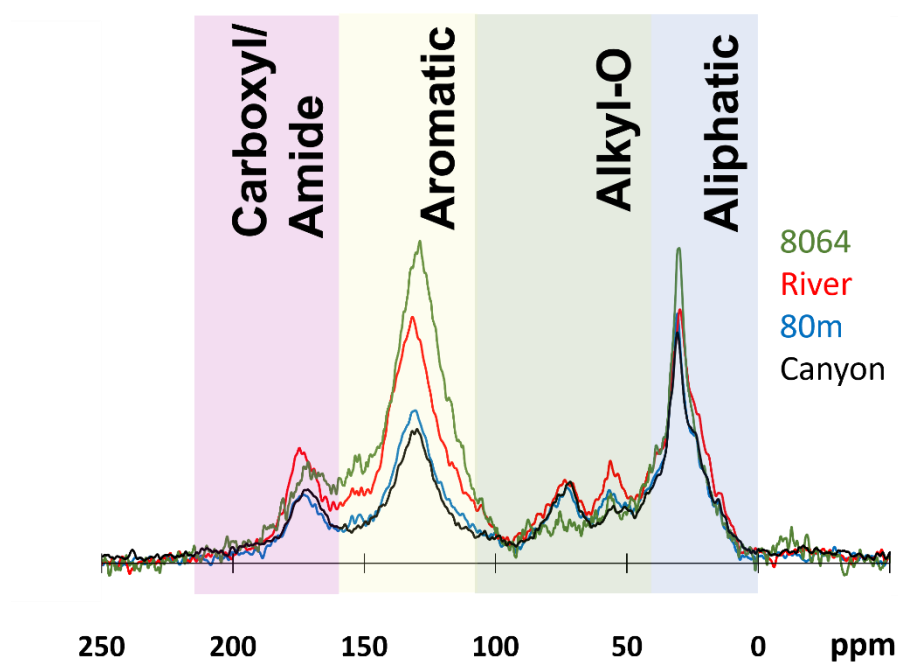


Fig. 2. Solid-state ^{13}C NMR spectra for 3 humic acid extracts from sediment along the transect; River, 80m, Canyon and a whole sediment sample collected near the mid-point of the transect for comparison, labeled as sample 8064.

Table 1. Sample names (listed by location or sediment depth below sea level), locations, % organic carbon (%C), % total nitrogen (%N), molar C/N, lambda 8 values, % organic carbon associated with humic acid (%C HA) fraction after alkaline extraction. Data included in this Table 13 previously reported by Sampere et al. (2008), with exception of %C HA, calculated from EA data.

Sample	Latitude	Longitude	% C	% N	C/N	Λ_8 (mg/100mg OC) ^a	% C HA ^b
River	29.2622	-89.3358	1.69	0.19	10.6	1.45	12.6
SW Pass	29.0630	-89.3073	1.99	0.20	11.4	2.4	-
50m Prox	28.9300	-89.5065	1.65	0.19	10.2	1.1	-
80m	28.7988	-89.5379	1.46	0.18	9.6	1.0	14.1
95m	28.7338	-89.5962	1.46	0.17	10.0	0.85	-
110m	28.6627	-89.6617	1.29	0.15	10.0	0.60	-
Canyon	28.5272	-89.7997	1.49	0.18	9.5	0.40	18.3

^a Λ_8 , total weight in mg of the sum of the vanillyl, syringyl and cinnamyl phenols normalized to 100 mg of organic carbon (total lignin phenols mg/100 mg OC)

^b % humic acid carbon normalized to the organic carbon from EA measurements of its whole sample.

Based on the relative peak areas, a structural assignment program proposed by Baldock et al., (2004) parsed the NMR spectra into contributions for various biochemical compound classes. Figure 3 (data shown in Table S1) displays the relative proportions of “lipids”, lignin, carbohydrates, condensed aromatics, and proteins for the three samples along the transect. Condensed aromatic carbons, called “char” by Baldock et al. (2004), constitute the largest carbon contributors with values of 47% in the riverine sample and decreasing to 33% in the offshore canyon sample. This supports previous work, based on polycyclic aromatic hydrocarbons (PAHs) abundance and composition of PAHs along the primary depositional pathways of the Mississippi

plume, that suggested inputs of possible “black carbon” sources from the Mississippi River basin and adjacent shelf regions (Mitra and Bianchi, 2003). The “lipids” or aliphatic carbons constitute the next greatest percentage of structural components ranging from 26% in the river to 33% in the canyon. Carbohydrates and lignin make up 8.4-11% and 0.65-3.8% of the carbon respectively. Proteinaceous carbon constitutes invariantly about 20% of the total carbons.

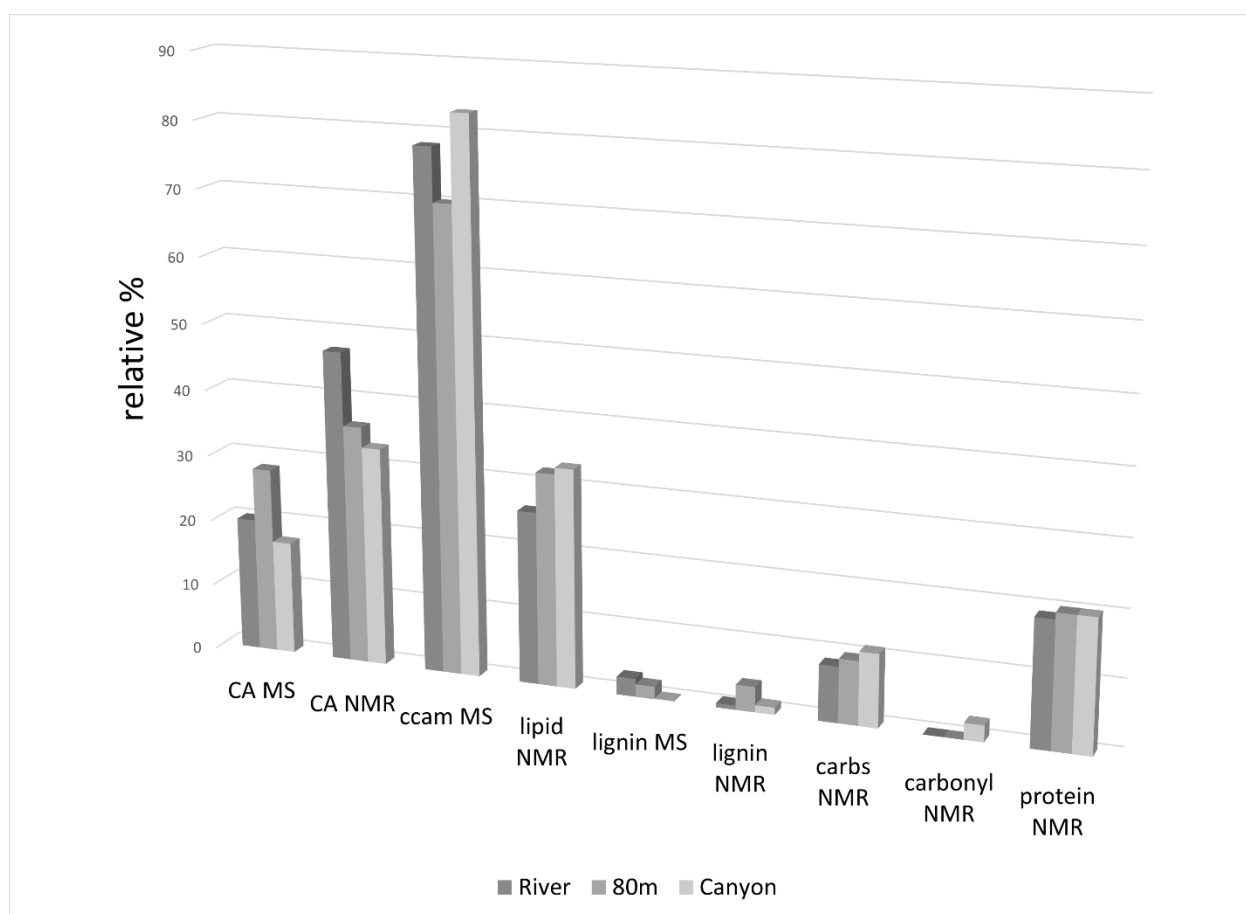


Fig. 3. Relative peak intensity percentages (r%) of molecular data for the HA extracts from FTICR-MS analysis (MS) and NMR peak data converted by the structural assignment software proposed by Baldock et al. (2004). Relative intensity from defined regions on the van Krevelen diagram MS data and relative intensity from NMR structural assignment software utilizing molecular mixing models, as proposed by Baldock et al. (2004).

FTICR-MS DATA

Van Krevelen diagrams (Van Krevelen, 1950, Kim et al. 2003) of the formulae obtained from FTICR-MS spectra of humic acids extracted from riverine and coastal sediments associated with the Mississippi/Atchafalaya system are shown to contain abundant series of aliphatic and aromatic molecules having multiple degrees of unsaturation (Fig. 4, 5).

The riverine sample (Fig. 4) is dominated by three clusters of molecular signatures as outlined by the boxes in all van Krevelen diagrams. Clusters are identified as lignin-like, condensed aromatics, and carboxyl containing aliphatic molecules (CCAM). Previous works have defined the general confines of these areas as follows; lignin-like molecules are typically found within H/C ratios ranging from 1.2 to 0.61 and O/C ratios ranging from 0.2 to 0.65 (Hockaday et al., 2009, Kim et al., 2004). Condensed aromatic structures are confined to H/C ratios ranging from 0.61 to 0.3 and O/C ratios ranging from 0.05 to 0.65 (Hertkorn et al., 2006), and have an aromaticity index (AI_{mod}) of ≥ 0.67 (Koch and Dittmar, 2006). Finally, a cluster of structures referred to as CCAM (DiDonato et al., 2016; Hartman et al., 2015) whose H/C and O/C values fall within 1.95 to 1.2 and 0.02 to 0.40, respectively. CCAM molecules appear to be ubiquitous components that appear in humic substances such as peats and coals, suggesting they may be the by-product of an environmentally processed microbial biomolecule (DiDonato et al., 2016). Alternatively, these aliphatic molecules may be derived from oxidative breakdown of lignin (Waggoner et al, 2015, Khatami et al., 2019).

As one progresses offshore towards the Mississippi Canyon, the samples collected along the transect out to 92 km distance and 540 m depth shows mass spectral peaks for humic acids that are fairly similar to those of the riverine sediment humic acids (Figs. 4 and 5). The predominantly

bimodal cluster of formulae for compounds in humic acids is similar in all samples along the transect (see supplemental data S3-S7), however diminishing signals are observed in the lignin region of the van Krevelen diagrams outward towards the canyon. Most noteworthy is the significant presence of formulae for condensed aromatic molecules which account for 17-20% of all peak intensities. This data is consistent with the NMR data that show a gradually diminishing proportion of aromatic signals along the transect towards the central Gulf of Mexico (Figures 2 and 3).

CHAPTER 4

DISCUSSION

NMR

Prior to discussing the molecular data, it is important to verify the relationship between the bulk chemical characteristics of OM and those of humic extracts. Fig. 2 shows solid-state ^{13}C NMR spectra of three humic acid extracts from the transect. Also shown is an NMR spectrum of the whole sediment collected separately from a site near the transect for comparison. It is immediately apparent that whole sediment and associated humic acids are similar with their composition of peaks mainly in aliphatic carbon regions (0-45 ppm for unsubstituted aliphatic carbons, 45-110 ppm for O and N-substituted alkyl carbons), aromatic carbons (110-160 ppm), and double-bonded oxygenated carbons (160-220 ppm for carboxyl, amide, ketone, and aldehyde carbon) (Fig. 2). The 8064-whole sediment sample spectrum being quite similar to that of the humic acids is suggestive that our approach of examining humic acids, a minor component of the sedimentary organic matter, is approximately reflecting the nature of the bulk sedimentary OM. It is noteworthy that the whole sediment spectrum does differ slightly from those of humic acids with regard to peaks for carboxyl/amide carbons (175 ppm) and O and N-substituted aliphatic carbons (45-100 ppm) commonly associated with carbohydrates and proteins. This is most likely attributable to the fact that a humic-acid extraction process can select for alkali-soluble structural entities that are more enriched in carboxyl/amide as well as aliphatic O- and N-containing structural functionalities such as oxidized carboxyl/hydroxyl-rich structures and proteinaceous materials. While this selectivity can provide misleading information on the overall structural nature of the organic matter, especially in instances such as soils where HA can be vastly different than the whole unextracted

sediment (Hatcher et al, 1983), the close similarity shown in Fig. 2 is indicative that structural differences are minor in this case.

The strong aliphatic peak in the whole sediment is understandably made up of not only terrigenous but also marine input, however this aliphatic peak is indicative of other terrigenous samples (Cook and Langford, 1998, Mao et al., 2010). The high proportion of aromatic carbon in all samples is a good indication that aromatic-rich soil-like material is an important component in both humic acids and whole sediment. There is also great similarity between humic acids along the transect and soil humic acids (Ikeya and Watanabe, 2016, Mao et al., 2017, Watanabe and Fujitake, 2008, Cook and Langford, 1998). The intense peak at 130 ppm for aromatic carbon is particularly noteworthy, as it has often been attributed to the presence of condensed aromatic structures found in combustion-derived black carbon (Kramer et al., 2004, Watanabe and Fujitake, 2008). Other major peaks in the spectra of soil humic acids are aliphatic signals presumably derived from lipid-like material in soils. Recent work by DiDonato and Hatcher (2017) attributes this aliphatic signal as a component of humic substances in soils more specifically, mainly alicyclic structural entities suggestive of CCAM. Thus, soil humic acids contain substantial amounts of these structural entities that can also be part of OM exported downriver and to the Gulf of Mexico. This further supports previous work by Goñi et al. 1997, 1998; Bianchi et al. 2011a; Sampere et al. 2008; and Waterson and Canuel 2008, that a significant amount of soil OM is being deposited in shelf-slope regions off the Mississippi/Atchafalaya system. To our knowledge, this is the first evidence showing a direct high-resolution bulk chemical structural signature that links soil OM from a typical mid-western USA soil to margin sediments within the primary depositional pathway of Mississippi/Atchafalaya plume deposits (McKee et al., 2004).

Lignin from terrigenous vascular plants typically shows characteristic signals in solid-state ^{13}C NMR spectra at 56 and 150 ppm. These are very weak in the spectra of Figure 2, consistent with what is observed for highly oxidized soil humic acids (Kramer et al., 2004, Watanabe and Fujitake, 2008) and soil OM (Thevenot et al., 2013). Goñi et al. (1998) and Sampere et al. (2008) both noted the low amounts of lignin phenols in sediments in offshore regions of the Mississippi/Atchafalaya system. Sampere et al. (2008) attributed this to the decay of lignin during transport, as reflected in the increasing acid/aldehyde (Ad/Al) ratios, an indicator of lignin decay (Bianchi 2011b), with distance offshore. Less oxidized peats typically have humic acids showing intense signals for lignin-derived OM (Hartman et al., 2015, Orem and Hatcher, 1987, Wang et al., 2011), owing to the anoxic conditions typically associated with peats. The virtual lack of such signals in solid-state ^{13}C NMR spectra of samples from the transect suggests that peat-derived OM from the lowland of the Mississippi Delta Complex is not a significant contributor to offshore sediments, which supports previous lignin-phenol work that suggests much of the marsh soil inputs are within the shallow inner-shelf region (Bianchi, 2011c). Alternatively, peat soils could be contributors, but their organic components have been altered significantly during export to the main channel of the river and the open shelf and are no longer recognizable as such (Wang et al., 2011).

Photochemical reactivity and microbial degradation also need to be taken into account when discussing the diagenetic state of OM in rivers and oceans. The role of microbial decay has not been fully demonstrated as the mechanism of primary lignin decay during transport offshore (Opsahl and Benner, 1998; Sampere et al., 2008). Opsahl and Benner (1998) found that when water samples containing high molecular weight (HMW) lignin from the Mississippi River was exposed to solar radiation, 80% degraded to low molecular weight (LMW) lignin molecules. Terrestrial organic matter is exposed to the greatest amount of solar radiation in river plumes at deltaic and

tributary interfaces with larger bodies of water like oceans (Opsahl and Benner, 1998, Dagg et al., 2004). Additionally, Opsahl and Benner (1998) found that dark control samples showed a decrease of HMW lignin of only 16% and attributed this to microbial degradation or adhesion to the experimental container. The remaining fraction of dissolved lignin proved more resistant to photochemical and microbial degradation. This data indicates that only a fraction of *terrOM* exported from rivers makes its way beyond coastal sediments and that microbial degradation in the water column and sediments plays an even smaller role. Goñi et al. (1998) state that the higher syringyl/vanillyl and cinnamyl/vanillyl ratios in shelf sediments indicates degradation occurs prior to deposition on the shelf as opposed to *in situ* decay. It should also be noted that there was no significant change in lignin biomarker composition of resuspended POM exposed to solar radiation in the shallow waters of the Mississippi River delta (Mayer et al., 2009).

Humic acid samples become less aromatic and more aliphatic with increasing distance offshore, a trend expected with additional marine inputs, and supported by plant pigments and fatty acids in sediments (Hedges et al., 1992, Sampere et al., 2008, Waterson and Canuel, 2008). Quantitative estimates of the relative proportions of carbon types are shown in Figure 6. From this it is evident that aliphatic carbons increase at the expense of aromatic carbons as one progresses offshore. The relative proportions of other peaks remain comparatively constant as the aromatic and aliphatic carbons fluctuate in relative proportions. The aliphatic and carbonyl peaks increase with increasing distance from shore, while the aromatic-C, C=C, and aromatic-O areas decrease. The decreasing areas correlate with that of a lignin signature, further supporting the findings of Goñi et al. (1997, 1998) and Sampere et al. (2008). One could reason that the increasing of the aliphatic peak could indicate mixing of marine input to the sediments or simply a dilution of *terrOM* over a vast area through hydrodynamic sorting as the distance from shore increases. However, as previously

discussed above and reported by Sampere et al. (2008), there is a significant increase in the Ad/Al ratios and a marked decrease of Λ_8 with distance indicating lignin decay is the main causative agent for the observed trend.

ESI-FTICR-MS

Van Krevelen diagrams (Van Krevelen, 1950, Kim et al., 2003) of the formulae obtained from FTICR-MS spectra have been used to show groupings of types of molecules by plotting O/C ratio on the ordinate against H/C ratios on the abscissa. Here we use the humic acids extracted from riverine and coastal sediments associated with the Mississippi/Atchafalaya system to show an abundant series of aliphatic and aromatic molecules with multiple degrees of unsaturation (Fig. 4 & 5).

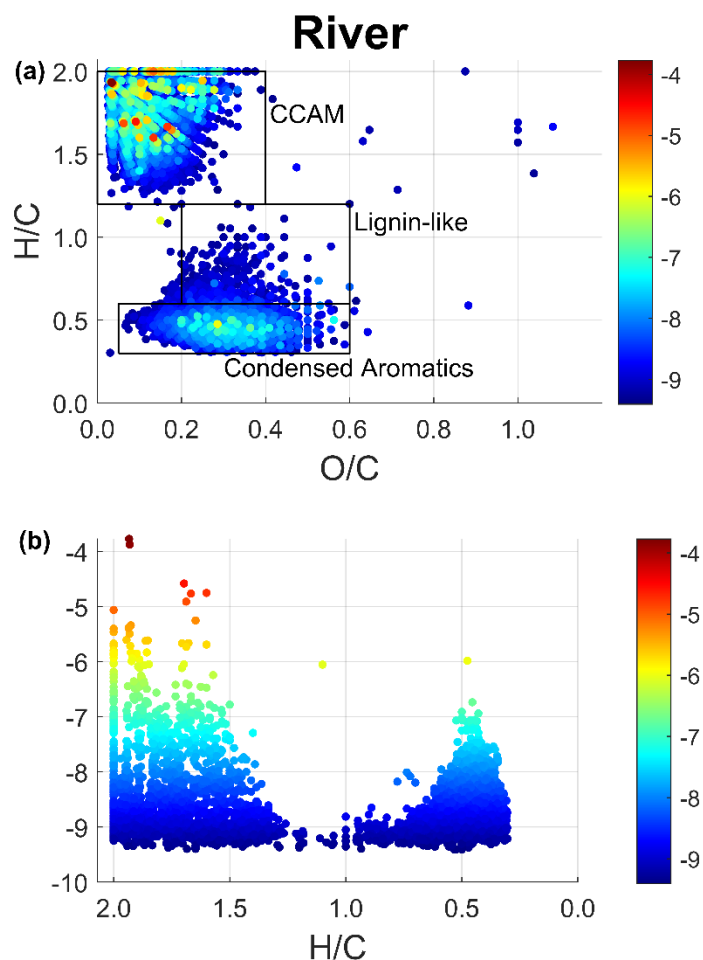


Fig. 4 Negative ion ESI-FTICR-MS data for humic acid extracts at the mouth of the river sample. The van Krevelen plot includes a log scale of relative intensities indicated by the color bar. (a) includes focus boxes around the CCAM, Lignin-like, and Condensed Aromatics regions as described in section 3.3 above to aid in visualization between samples. (b) shows the same magnitude plot from the H/C axis viewpoint allowing better visualization of the intensities for the aforementioned regions.

The riverine sample (Fig. 4) is dominated by three clusters of molecular signatures, as can be seen in the boxed areas of the van Krevelen diagrams labeled as CCAM, Lignin-like, and Condensed Aromatics. The distribution of molecules is quite distinct from dissolved OM (Chen et al., 2014,

Koch and Dittmar, 2006, Lu et al., 2015) but is typical for humic acids from soils (Didonato et al., 2016, Ikeya et al., 2015). DiDonato et al. (2016) analyzed Catlin humic acids from Ogle, IL (soil HA) which constitutes part of the Mississippi River catchment. DiDonato et al. (2016) determined that the condensed aromatic formulae represented 17% of the total magnitude of all peaks in the spectrum for this humic acid, while 78% of formulae were attributed to CCAM formulae and 3% were lignin-like.

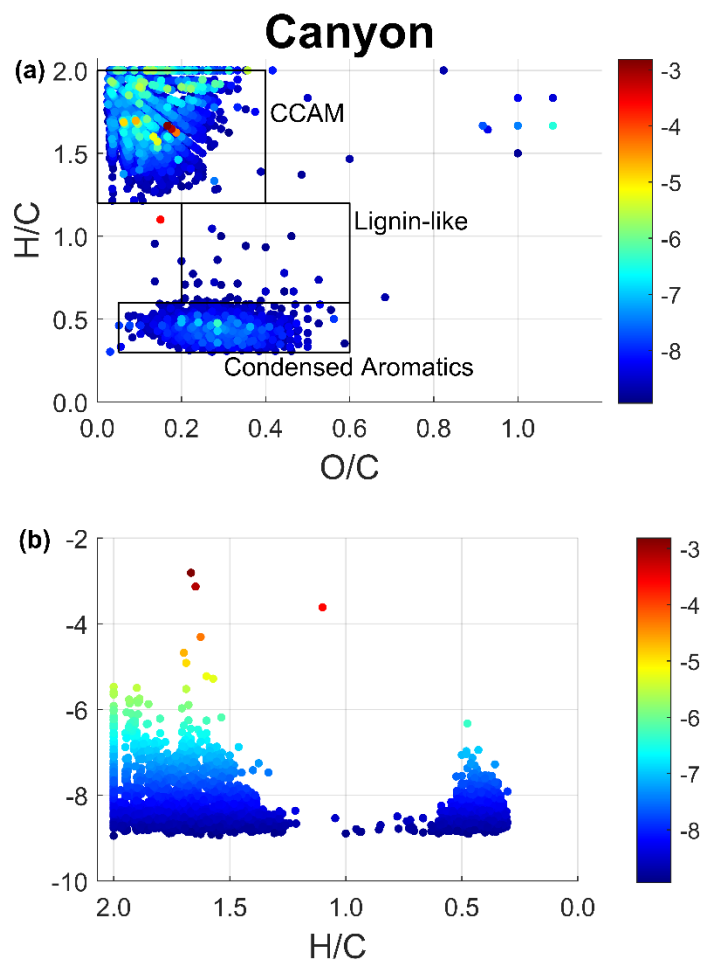


Fig. 5. Negative ion ESI-FTICR-MS data for humic acid extracts of the canyon sample. The van Krevelen plot includes a log scale of relative intensities indicated by the color bar. (a) includes focus boxes around the CCAM, Lignin-like, and Condensed Aromatics regions as described in section 3.3 above to aid in visualization between samples. (b) shows the same magnitude plot from the H/C axis viewpoint allowing better visualization of the intensities for the regions previously mentioned.

A great similarity is observed between the HA soil samples reported by DiDonato et al., (2016) and both the riverine and canyon samples indicating a commonality of source. Fig. 4b & 5b, displays a projection of peak magnitudes as viewed from the H/C (y-axis) versus the log relative intensity (z-axis) indicating that the CCAM and condensed aromatic clusters are present in

substantial proportions. Summing the peak magnitudes for molecules that plot within each of the cluster areas defined above and shown conceptually in Figure S8, we calculate the relative proportion of mass spectral peak magnitude for each of the clusters (Figure 6). For the riverine sample, CCAM formulae are the largest magnitude contributors, accounting for 78% of all CHO peaks. The condensed aromatics contribute 20% and lignin contributes 2.7%, Figure 6. These values match well with those measured by DiDonato et al. (2016) for the Catlin soil HA sample mentioned above.

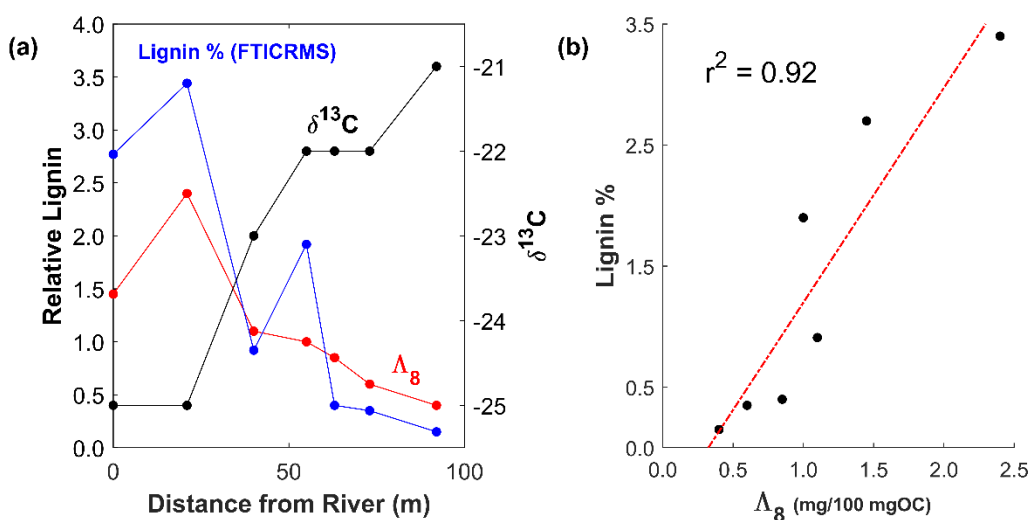


Fig.6. (a) Λ_8 values (mg lignin/ 100mg organic carbon) from CuO oxidation analysis and stable carbon isotopic composition for the whole sediment measured by Sampere et al. (2008), lignin % from FTICR-MS data (summation of peak magnitudes for lignin-like formulae.) (b) correlation between Λ_8 values and lignin % from mass spectral data.

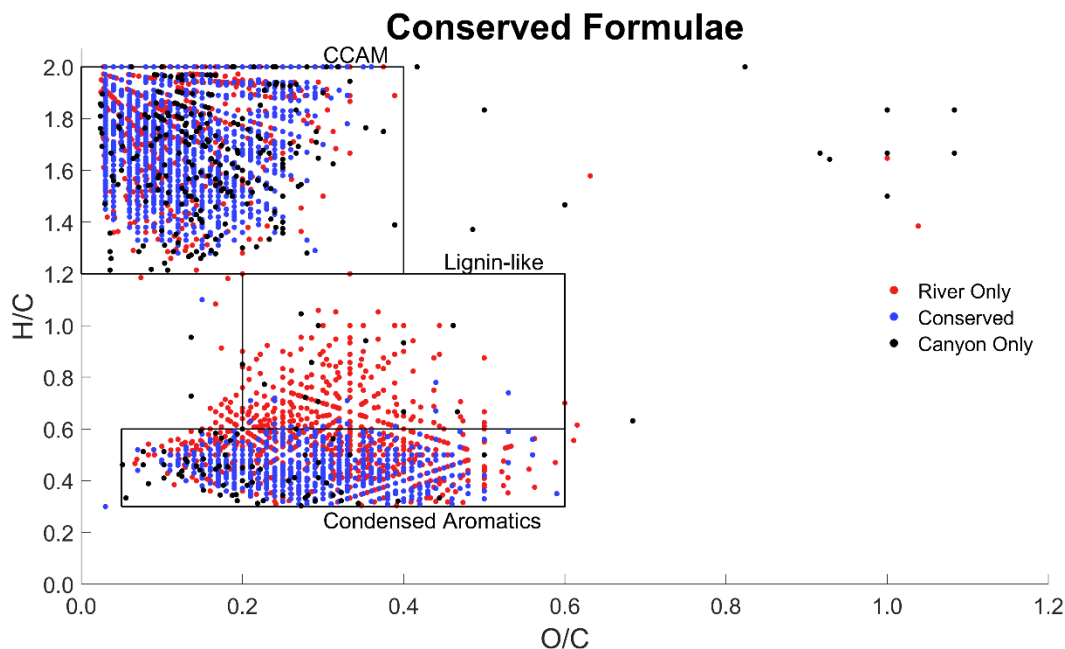


Fig. 7. Comparison of the formulae between the river and the canyon. Formulae unique to the river and canyon only represent 38% and 15% respectively. Meaning the majority of the formulae persist from the river to the canyon, a distance of 92 km and a depth of 540 m.

This result is quite surprising for samples expected to contain a great diversity of molecular types, given that one might expect source materials in riverine sediments to be diverse in origin. The principally bimodal distribution of all molecular formulae suggests that source diversity is limited and is mainly composed of OM from oxidized soils. This clustering phenomenon has also been observed in soil humic acids (Ikeya et al., 2015). Most notably, N-containing formulae (CHON and CHONS) plot in the condensed aromatic and aliphatic/alicyclic carbon regions. Those formulae plotting in the aliphatic region could likely be molecules derived from proteinaceous material even though one might expect proteinaceous material to plot at higher O/C ratios due to the presence of amide functionality. Some of the N-containing formulae could be non-proteinaceous. The formulae containing CHOS atoms are the exception to what is noted above.

These formulae plot mostly in the protein-like region of the van Krevelen diagram with a few formulae in what is known as the carbohydrate region (Kim et al., 2004). Sulfur addition to carbohydrates has been noted previously (Sinninghe Damsté et al., 1995), so it is possible that these formulae are sulfurized carbohydrate-like compounds. However, increasing the number of allowed sulfur atoms in the Matlab formula assignment software did not populate new sulfur containing formulae.

Another interesting result comes from the analysis of common versus unique assigned formulae (Fig. 7). About 1800 formulae are found to be common between the two samples, representing 62% of the river and 85% of the canyon assigned formulae. Further investigation of the peak intensities related to the common formulae shows that 82% of total river and 93% of total canyon intensities are represented. Given the fact that the formulae for both samples plot in much of the same regions lends more weight to the assumption that these molecules may have a common origin without much change in their chemical composition. Previous studies have shown selective degradation of DOM by way of physical protection (Arnarson and Keil, 2007, Wang et al., 2011), molecular/functional group recalcitrance (Gough et al., 1993, Hedges and Mann, 1979a, Kiem and Kögel-Knabner, 2003, Opsahl and Benner, 1997) and oxygen availability (Arnarson and Keil, 2007, Bianucci et al., 2018) to be possible causes for this preservation phenomenon.

The diminishing proportion of formulae that cluster in the lignin-like region of the van Krevelen diagram with progression towards the canyon is consistent with the trends in lignin phenol measurements made by Sampere et al. (2008). Fig. 6a shows plots of the percentage of mass spectral intensity in the lignin region with the lignin phenol data from Sampere et al. (2008) along the transect. Fig. 7b shows a high degree of co-variance of these two analyses with an excellent correlation between the two independent measurements. This correlation with a lignin phenol

measurement, considered to be quantitative, suggests that the FTICR-MS data are providing a quantitative or at least a semi-quantitative evaluation of the lignin contents of the samples. Note that the slope of this correlation is nearly 1:1.

Condensed aromatic formulae gradually diminish as one progresses offshore while CCAM formulae increase in this direction, as can be seen in the van Krevelen diagram of the canyon in Fig. 4a and Figure 5. We could easily attribute this to mixing of the soil-derived OM with that derived from autochthonous sources enriched in CCAM-like formulae. Ogawa et al., 2001 have suggested that aliphatic formulae in FTICR-MS spectra are derived from autochthonous marine microbial biomass, which would also explain the increase of aliphatic signatures towards deeper ocean sediments.

CHAPTER 5

CONCLUSIONS

NMR and FTICR-MS data clearly show a trend as one traverses from the mouth of the Mississippi River to the offshore Mississippi Canyon. The humic acids and whole sediment appear to be influenced greatly by structural entities typically found in soils (e.g., aromatic molecules). The decreasing trend in condensed aromatic carbon and increased aliphatic 'lipid-like' carbon as one progresses offshore is consistent with a trend that can be derived from a simple two-end-member mixing of *terrOM* and autochthonous marine organic matter.

Alternatively, this trend of diminishing condensed aromatic character could arise from hydrodynamic sorting of humic material among fine and coarse fractions as suggested by Goñi et al. (1997) to explain the stable carbon isotope trends. Sampere et al. (2008) observed a similar carbon isotope trend for samples examined in this manuscript and shown in Fig. 6. In this scenario the finer particles, which would be transported further offshore, would need to be isotopically enriched in ^{13}C (presumably having more of a C_4 plant source) and relatively more enriched in CCAM formulae. Baldock et al. (1992) showed by solid-state ^{13}C NMR that the fine fractions of numerous soils were more enriched in aliphatic carbons than aromatic carbons, while medium sized fractions showed a more abundant aromatic signature. They attributed the aliphatic character to the increased presence of microbial biomass in soil. Thus, if soil is a major source of organic matter to the Gulf of Mexico and hydrodynamic sorting of exported particles from soils were taking place, one would observe that the finer fractions would be transported further offshore and that these would be enriched in aliphatic constituents; a trend observed with both NMR studies and the FTICR-MS data presented here. For this scenario to agree with the trends in carbon isotope data, the fine fractions of the soil would need to be enriched in ^{13}C relative to the coarser fraction.

Balesdent et al. (1988) showed that the fine fractions of soil in some soil plots of native prairie soils from the Mississippi catchment are isotopically enriched in ^{13}C compared to coarser fractions of the soil and compared to soils developed from C_3 plants. Thus, we find this scenario quite feasible as an explanation for the trends observed in the Mississippi Delta. It is important to note that these trends, while present in some of the shallower regions of the shelf, are more clearly explainable as linked with mid-western soil for the deeper water, since inputs from eroding local coastal marshes (with C_4 plants) to inner shelf sites can complicate trends of C_4 plants inputs (Bianchi, 2011c).

Finally, we offer a third explanation for the decreasing trend in condensed aromatic carbons and increased aliphatic ‘lipid-like’ carbons as one progresses offshore. The diminishing proportion of aromatic structures towards the offshore canyon could reflect a selective oxidative trend, especially if reactive oxygen species were responsible for degradation and a greater exposure of sediments to oxidation occurs towards the offshore. This supports previous studies of lignin phenols (Goñi et al., 1997, Goñi et al., 1998, Sampere et al., 2008) that show more heavily oxidized lignin as one progresses offshore. It is also known that oxidative processes involving reactive oxygen species such as hydroxyl radical or singlet oxygen can decompose aromatic structures selectively compared with aliphatic structures (Stubbins et al., 2010, Waggoner et al., 2017). Condensed aromatic molecules have been shown to be readily oxidized by hydroxyl radicals, either driven by photochemistry (Chen et al., 2014, Stubbins et al., 2010), or by oxidative enzymes (Bezalel et al., 1996). CCAM-type molecules, however, have recently been shown to be less prone to oxidative degradation which mainly involves an increase in oxygen functional groups (Waggoner et al., 2017). Thus, one could envision that the offshore sediments that are most likely more oxidized due to continued resuspension and redeposition would lose their aromatic structural entities

preferentially to the aliphatic structures. More research is needed to show a possible pathway for this explanation. It is not known whether selective oxidation of aromatic structures induces an isotopic fractionation leading to OM more enriched in ^{13}C . In light of sea-level rise contributing to *terr*OM decay at the coastal margins, further investigations should be made to better understand the mechanisms that contribute to the fate of OM, be it burn off or conversion.

REFERENCES

- Aller, R.C. Mobile deltaic and continental shelf muds as suboxic, fluidized bed reactors. *Mar. Chem.* **1998**, 61, 143-155.
- Allison M.A., Bianchi T.S., McKee B.A. and Sampere T.P. Carbon burial on river-dominated continental shelves: Impact of historical changes in sediment loading adjacent to the Mississippi River. *Geophys. Res. Lett.* **2007**, 34, DOI:10.1029/2006GL028362.
- Arnarson T.S. and Keil R.G. Changes in organic matter–mineral interactions for marine sediments with varying oxygen exposure times. *Geochim. Cosmochim. Acta* **2007**, 71, 3545-3556.
- Baldock J.A., Masiello C.A., G  linas Y. and Hedges J.I. Cycling and composition of organic matter in terrestrial and marine ecosystems. *Mar. Chem.* **2004**, 92, 39-64.
- Bladock J.A., Oades J.M., Waters A.G., Peng X., Vassallo A.M. and Wilson M.A. Aspects of the chemical structure of soil organic materials as revealed by solid-state ¹³C NMR spectroscopy. *Biogeochem.* **1992**, 16(1), 1-42
- Balesdent J., Wagner G.H. and Mariotti A. Soil Organic Matter Turnover in Long-term Field Experiments as Revealed by Carbon-13 Natural Abundance. *Soil Sci. Soc. Am.* **1988**, J. 52, 118-124.
- Berner R.A. Biogeochemical cycles of carbon and sulfur and their effect on atmospheric oxygen over phanerozoic time. *Palaeogeogr. Palaeoclimatol. Palaeoecol.* **1989**, 75, 97-122.
- Bezalel, L., Hadar, Y. and Cerniglia, C.E. Mineralization of Polycyclic Aromatic Hydrocarbons by the White Rot Fungus *Pleurotus ostreatus*. *Appl. Environ. Microbiol.* **1996**, 62(1), 292-295.
- Bianchi T.S. The role of terrestrially derived organic carbon in the coastal ocean: a changing paradigm and the priming effect. *Proc. Natl. Acad. Sci.* **2011a**, U.S.A. SA 108, 19473.
- Bianchi T.S. and Canuel E.A. In *Chemical Biomarkers in Aquatic Ecosystems*. Princeton University Press, **2011b**; pp 263-265.
- Bianchi T.S., Galler J.J. and Allison M.A. Hydrodynamic sorting and transport of terrestrially derived organic carbon in sediments of the Mississippi and Atchafalaya Rivers. *Estuar. Coast. Shelf Sci.* **2007**, 73, 211-222.
- Bianchi T.S., Mitra S. and McKee B. Sources of terrestrially derived carbon in the Lower Mississippi River and Louisiana shelf: Implications for differential sedimentation and transport at the coastal margin. *Mar. Chem.* **2002**, 77, 211-223
- Bianchi T.S., Wysocki L.A., Schneider K.M., Filley T.R., Corbett D.R. and Kolker A. Sources of terrestrial organic carbon in the Louisiana shelf (USA): Evidence for the importance of coastal marsh inputs. *Aquat. Geochem.* **2011c**, 17, 431-456.
- Bianucci L., Balaguru K., Smith R.W., Leung L.R. and Moriarty J.M. Contribution of hurricane-induced sediment resuspension to coastal oxygen dynamics. *Sci. Rep.* **2018**, 8, 15740.
- Blair N.E. and Aller R.C. The Fate of Terrestrial Organic Carbon in the Marine Environment. *Ann. Rev. Mar. Sci.* **2011**, 4, 401-423.
- Blattmann T.M., Liu Z., Zhang Y., Zhao Y., Haghipour N., Montlu  on D.B., Pl  tze M. and Eglinton T.I. Mineralogical control on the fate of continentally derived organic matter in the ocean. *Science* **2019**, 366, 742.
- Chen H.M., Abdulla H., Sanders R., Myneni S., Mopper K. and Hatcher P.G. Production of Black Carbon-like and Aliphatic Molecules from Terrestrial Dissolved Organic Matter in the Presence of Sunlight and Iron. *Environ. Sci. Technol. Lett.* **2014**, 1, 399-404.

- Cook R. L., Langford C. H., Structural Characterization of a Fulvic Acid and a Humic Acid Using Solid-State Ramp-CP-MAS ^{13}C Nuclear Magnetic Resonance. *Environ. Sci. Technol.* **1998**, 32 (5), 719-725.
- Dagg M., Benner R., Lohrenz S. and Lawrence D. Transformation of dissolved and particulate materials on continental shelves influenced by large rivers: plume processes. *Cont. Shelf Res.* **2004**, 24, 833-858.
- De la Rosa, J. M.; González-Pérez, J. A.; González-Vila, F. J.; Knicker, H.; Araújo, M. F. Molecular composition of sedimentary humic acids from South West Iberian Peninsula: A multi-proxy approach. *Org. Geochem.* **2011**, 42 (7), 791-802.
- Didonato N., Chen H., Waggoner D. and Hatcher P.G. Potential origin and formation for molecular components of humic acids in soils. *Geochim. Cosmochim. Acta* **2016**, 178, 210-222.
- Didonato N. and Hatcher P.G. Alicyclic carboxylic acids in soil humic acid as detected with ultrahigh resolution mass spectrometry and multi-dimensional NMR. *Org. Geochem.* **2017**, 112, 33-46.
- Giosan L., Syvitski J., Constantinescu S. and Day J. Climate change: protect the world's deltas. *Nature* **2014**, 516, 31-33.
- Goñi M.A., Ruttenberg K. and Eglinton T. Source and contribution of terrigenous organic carbon to surface sediments in the Gulf of Mexico. *Nature* **1997**, 389, 275-278.
- Goñi M.A., Ruttenberg K.C. and Eglinton T.I. A reassessment of the sources and importance of land-derived organic matter in surface sediments from the Gulf of Mexico. *Geochim. Cosmochim. Acta* **1998**, 62, 3055-3075.
- Gordon, Elizabeth S., Goñi, Miguel A. Sources and distribution of terrigenous organic matter delivered by the Atchafalaya River to sediments in the northern Gulf of Mexico. *Geochim. et Cosmochim. Acta*, **2003**, 67 (13). 2359-2375
- Gordon E.S. and Goñi M.A. Controls on the distribution and accumulation of terrigenous organic matter in sediments from the Mississippi and Atchafalaya river margin. *Mar. Chem.* **2004**, 92, 331-352.
- Gough M.A., Fauzi R., Mantoura C. and Preston M. Terrestrial plant biopolymers in marine sediments. *Geochim. Cosmochim. Acta* **1993**, 57, 945-964.
- Grinhut, T., Hertkorn, N., Schmitt-Kopplin, P., Hadar, Y. and Chen, Y. Mechanisms of Humic Acids Degradation by White Rot Fungi Explored Using ^1H NMR Spectroscopy and FTICR Mass Spectrometry. *Environ. Sci. Technol* **2011**, 45, 2748-2754.
- Hartman B.E., Chen H. and Hatcher P.G. A non-thermogenic source of black carbon in peat and coal. *Int. J. Coal Geol.* **2015**, 144-145, 15-22.
- Hatcher P.G. The origin, composition, chemical structure, and diagenesis of humic substances, coals, and kerogens as studied by nuclear magnetic resonance., Ph.D. dissertation University of Maryland, 1980 (Ed.).
- Hatcher P.G., Breger I.A., Dennis L.W. and Maciel G.E. Solid-state ^{13}C NMR of sedimentary humic substances; new revelations on their chemical composition, in Christman, R.F. and Gjessing, E.T., eds., Aquatic and Terrestrial Humic Materials. Ann Arbor, MI, Ann Arbor Science, 1983, p. 37-81.
- Hedges J. and Oades J. Comparative organic geochemistries of soils and marine sediments, *Org. Geochem.* **1997a**, 27 (7/8), pp. 319-361.
- Hedges J.I., Cowie G.L., Richey J.E., Quay P.D., Benner R., Strom M. and Forsberg B.R. Origins and processing of organic matter in the Amazon River as indicated by carbohydrates and amino acids. *Limnol. Oceanogr.* **1994**, 39, 743-761.

- Hedges J.I., Hatcher P.G., Ertel J.R. and Meyers-Schulte K.J. A comparison of dissolved humic substances from seawater with Amazon River counterparts by ^{13}C -NMR spectrometry. *Geochim. Cosmochim. Acta* **1992**, 56, 1753-1757.
- Hedges J.I. and Keil R.G. Sedimentary organic matter preservation: an assessment and speculative synthesis. *Mar. Chem.* **1995**, 49, 81-115.
- Hedges J.I. and Mann D.C. The characterization of plant tissues by their lignin oxidation products. *Geochim. Cosmochim. Acta* **1979a**, 43, 1803-1807.
- Hedges J.I. and Oades J.M. Comparative organic geochemistries of soils and marine sediments. *Org. Geochem.* **1997b**, 27, 319-361.
- Hedges J.I. and Parker P.L. Land-derived organic matter in surface sediments from the Gulf of Mexico. *Geochim. Cosmochim. Acta* **1976**, 40, 1019-1029.
- Hernes P.J., Kaiser K., Dyda R.Y. and Cerli C. Molecular Trickery in Soil Organic Matter: Hidden Lignin. *Environ. Sci. Technol* **2013**, 47, 9077-9085.
- Hertkorn N., Benner R., Frommberger M., Schmitt-Kopplin P., Witt M., Kaiser K., Ketrup A. and Hedges J.I. Characterization of a major refractory component of marine dissolved organic matter. *Geochim. Cosmochim. Acta* **2006**, 70, 2990-3010.
- Hertkorn, N., Harir, M., Cawley, K.M., Schmitt-Kopplin, P. and Jaffé, R. Molecular characterization of dissolved organic matter from subtropical wetlands: a comparative study through the analysis of optical properties, NMR and FTICR/MS. *Biogeosciences* **2016**, 13, 2257-2277.
- Hockaday W., Purcell J., Marshall A.G., Baldock J. and Hatcher P.G. Electrospray and photoionization mass spectrometry for the characterization of organic matter in natural waters: a qualitative assessment. *Org. Geochem. Limnol. Oceanogr. Methods* **2009**, 7, 81-95.
- Ikeya K., Sleighter R.L., Hatcher P.G. and Watanabe A. Characterization of the chemical composition of soil humic acids using Fourier transform ion cyclotron resonance mass spectrometry. *Geochim. Cosmochim. Acta* **2015**, 153, 169-182.
- Ikeya K. and Watanabe A. Application of ^{13}C ramp CPMAS NMR with phase-adjusted spinning sidebands (PASS) for the quantitative estimation of carbon functional groups in natural organic matter. *Anal Bioanal Chem* **2016**, 408, 651-655.
- Johnson R.L. and Schmidt-Rohr K. Quantitative solid-state ^{13}C NMR with signal enhancement by multiple cross polarization. *J. Magn. Reson.* **2014**, 239, 44-49.
- Khatami S., Deng Y., Tien M., and Hatcher P.G. Lignin contribution to aliphatic constituents of humic acids through fungal degradation. *J. of Environ. Qual.* **2019**, 48 (6), 1565-1570.
- Kiem R. and Kögel-Knabner I. Contribution of lignin and polysaccharides to the refractory carbon pool in C-depleted arable soils. *Soil Biol. Biochem.* **2003**, 35, 101-118.
- Kim S., Kaplan L.A., Benner R. and Hatcher P.G. Hydrogen-deficient molecules in natural riverine water samples evidence for the existence of black carbon in DOM. *Mar. Chem.* **2004**, 92, 225-234.
- Kim S., Kramer R.W., Hatcher P.G. Graphical method for analysis of ultrahigh-resolution broadband mass spectra of natural organic matter, the van Krevelen diagram. *Anal. Chem.* **2003**, 75, 5336-5344.
- Kirchman D. and Suzuki Y. High Turnover Rates of Dissolved Organic Carbon During a Spring Phytoplankton Bloom. *Nature* **1991**, 352, 612.
- Klotzbücher T., Kalbitz K., Cerli C., Hernes P. J., and Kaiser K. Gone or just out of sight? The apparent disappearance of aromatic litter components in soils. *SOIL* **2016**, 2, 325–335

- Koch B.P. and Dittmar T. From mass to structure: an aromaticity index for high-resolution mass data of natural organic matter. *Rapid Commun. Mass Spectrom.* **2006**, 20, 926-932.
- Kramer R.W., Kujawinski E.B. and Hatcher P.G. Identification of Black Carbon Derived Structures in a Volcanic Ash Soil Humic Acid by Fourier Transform Ion Cyclotron Resonance Mass Spectrometry. *Environ. Sci. Technol.* **2004**, 38, 3387-3395.
- Kuliński, K., Hammer, K., Schneider, B. and Schultz-Bull, D. Remineralization of terrestrial dissolved organic carbon in the Baltic Sea. *Mar. Chem.* **2016**, 181, 10-17.
- Li M., Peng C., Wang M., Xue W., Zhang K., Wang K., Shi G, and Zhu Q. The carbon flux of global rivers: A re-evaluation of amount and spatial patterns. *Ecol. Indic.* **2017**, 80, 40-51
- Lu Y., Li X., Mesfioui R., Bauer J.E., Chambers R.M., Canuel E.A. and Hatcher P.G. Use of ESI-FTICR-MS to Characterize Dissolved Organic Matter in Headwater Streams Draining Forest-Dominated and Pasture-Dominated Watersheds. *PLoS One* **2015**, 10, e0145639.
- Mao J., Cao X., Olk D.C., Chu W. and Schmidt-Rohr K. Advanced solid-state NMR spectroscopy of natural organic matter. *Prog. Nucl. Magn. Reson. Spectrosc.* **2017**, 100, 17-51.
- Mao J., Palazzo A.J., Olk D.C., Clapp C.E., Senesi N., Bashore T.L., Cao X. Chemical Structure of Soil Organic Matter in Slickspots as Investigated by Advanced Solid-State NMR. *Soil Sci* **2010**, 175 (7), 329-338.
- Mayer L.M., Schick L.L., Bianchi T.S. and Wysocki L.A. Photochemical changes in chemical markers of sedimentary organic matter source and age. *Mar. Chem.* **2009**, 113, 123-128.
- Mayorga E., Aufdenkampe A.K., Masiello C.A., Krusche A.V., Hedges J.I., Quay P.D., Richey J.E. and Brown T.A. Young organic matter as a source of carbon dioxide outgassing from Amazonian rivers. *Nature* **2005**, 436, 538-541.
- McKee B.A., Aller R.C., Allison M.A., Bianchi T.S. and Kineke G.C. Transport and transformation of dissolved and particulate materials on continental margins influenced by major rivers: benthic boundary layer and seabed processes. *Cont. Shelf Res.* **2004**, 24, 899-926.
- Mead R. and Goñi M.A. A lipid molecular marker assessment of sediments from the Northern Gulf of Mexico before and after the passage of Hurricane Lili. *Org. Geochem.* **2006**, 37, 1115-1129.
- Middelburg J.J., Vlug T. and Jaco W.A. van der Nat F. Organic matter mineralization in marine systems. *Glob Planet Change* **1993**, 8, pp. 47-58.
- Mitra S. and Bianchi T.S. A preliminary assessment of polycyclic aromatic hydrocarbon distributions in the lower Mississippi River and Gulf of Mexico. *Mar. Chem.* **2003**, 82, 273-288.
- Moriarty J.M., Harris C.K., Friedrichs M.A.M., Fennel K. and Xu K. Impact of Seabed Resuspension on Oxygen and Nitrogen Dynamics in the Northern Gulf of Mexico: A Numerical Modeling Study *J. Geophys. Res. Oceans* **2018**, 123, 7237-7263.
- Nelson P.N. and Baldock J.A. Estimating the molecular composition of a diverse range of natural organic materials from solid-state ¹³C NMR and elemental analyses. *Biogeochem.* **2005**, 72, 1-34
- Obeid W. Investigation of the potential for algae to produce hydrocarbon based fuels from algae by hydrous pyrolysis, Ph.D. Dissertation, Old Dominion University, Norfolk, VA, 2015.
- Ogawa H., Amagai Y., Koike I., Kaiser K. and Benner R. Production of refractory dissolved organic matter by bacteria. *Science (Washington)* **2001**, 292, 917-920.

- Opsahl S. and Benner R. Distribution and cycling of terrigenous dissolved organic matter in the ocean. *Nature* (London) **1997**, 386, 480-482.
- Opsahl S. and Benner R. Photochemical reactivity of dissolved lignin in river and ocean waters. *Limnol. Oceanogr. Oceanogr* **1998**, 43, 1297-1304.
- Orem W.H. and Hatcher P.G. Early diagenesis of organic matter in a Sawgrass peat from the Everglades, Florida. *Int. J. Coal Geol.* **1987**, 8, 33-54.
- Prahl F.G., Ertel J.R., Goni M.A., Sparrow M.A. and Eversmeyer B. Terrestrial organic carbon contributions to sediments on the Washington margin. *Geochim. Cosmochim. Acta* **1994**, 58, 3035-3048.
- Sampere T.P., Bianchi T.S., Wakeham S.G. and Allison M.A. Sources of organic matter in surface sediments of the Louisiana Continental margin: Effects of major depositional/transport pathways and Hurricane Ivan. *Cont. Shelf Res.* **2008**, 28, 2472-2487.
- Schlesinger W.H. and Melack J.M. Transport of organic carbon in the world's rivers. *Tellus* **1981**, 33, 172-187.
- Shields M., Bianchi T., Mohrig D., Hutchings J., Kenney W., Kolker A. and Curtis J. Carbon storage in the Mississippi River delta enhanced by environmental engineering. *Nat. Geosci.* **2017**, 10, 846-851.
- Sinninghe Damsté J.S., Kenig F., Koopmans M.P., Köster J., Schouten S., Hayes J.M. and de Leeuw J.W. Evidence for gammacerane as an indicator of water column stratification. *Geochim. Cosmochim. Acta* **1995**, 59, 1895-1900.
- Sleighter R.L. and Hatcher P.G. The application of electrospray ionization coupled to ultrahigh resolution mass spectrometry for the molecular characterization of natural organic matter *J. Mass Spectrom.* **2007**, 42, 559-574.
- Sleighter R.L. and Hatcher P.G. Molecular characterization of dissolved organic matter (DOM) along a river to ocean transect of the lower Chesapeake Bay by ultrahigh resolution electrospray ionization Fourier transform ion cyclotron resonance mass spectrometry *Mar. Chem.* **2008**, 110, 140-152.
- Smith S.V. and Mackenzie F.T. The ocean as a net heterotrophic system: Implications From the carbon biogeochemical cycle *Global Biogeochem. Cycles* **1987**, 1, 187-198.
- Stubbins A., Spencer R., Chen H.M., Hatcher P.G., Mopper K., Hernes, P., Mwamba V., Mangangu A., Wabakanghanzi J. and Six J. Illuminated darkness: Molecular signatures of Congo River dissolved organic matter and its photochemical alteration as revealed by ultrahigh precision mass spectrometry. *Limnol. Oceanogr. Oceanogr* **2010**, 55, 1467-1477.
- Sugimura Y. and Suzuki Y. A high-temperature catalytic oxidation method for the determination of non-volatile dissolved organic carbon in seawater by direct injection of a liquid sample. *Mar. Chem.* **1988**, 24, 105-131.
- Thevenot M., Dignac M.F., Mendez-Millan M., Bahri H., Hatté C., Bardoux G. and Rumpel C. Ligno-aliphatic complexes in soils revealed by an isolation procedure: implication for lignin fate. *Biol. Fertil. Soils* **2013**, 49, 517-526.
- Van Krevelen D. Graphical-statistical method for the study of structure and reaction processes of coal. *Fuel* **1950**, 29, 269-284.
- Waggoner, D.C., Chen, H., Willoughby, A.S. and Hatcher, P.G. Formation of black carbon-like and alicyclic aliphatic compounds by hydroxyl radical initiated degradation of lignin. *Org. Geochem* **2015**, 82, 69-76.

- Waggoner D.C., Wozniak A.S., Cory R.M. and Hatcher P.G. The role of reactive oxygen species in the degradation of lignin derived dissolved organic matter. *Geochim. Cosmochim. Acta* **2017**, 208, 171-184.
- Wakeham S.G., Canuel E.A., Lerberg E.J., Mason P., Sampere T.P. and Bianchi T.S. Partitioning of organic matter in continental margin sediments among density fractions *Mar. Chem.* **2009**, 115, 211-225.
- Wang J.J., Dodla S.K., DeLaune R.D., Hudnall W.H. and Cook R.L. Soil Carbon Characteristics in Two Mississippi River Deltaic Marshland Profiles. *Wetlands* **2011**, 31, 157-166.
- Watanabe A. and Fujitake N. Comparability of composition of carbon functional groups in humic acids between inverse-gated decoupling and cross polarization/magic angle spinning ^{13}C nuclear magnetic resonance techniques. *Anal. Chim. Acta* **2008**, 618, 110-115.
- Waterson E.J. and Canuel E.A. Sources of sedimentary organic matter in the Mississippi River and adjacent Gulf of Mexico as revealed by lipid biomarker and $\delta^{13}\text{C}$ TOC analyses. *Org. Geochem.* 39, **2008**, 422-439.
- Wu Y., Zhu K., Zhang J., Muller M., Jiang S., Mujahid A., Muhamad M.F. and Sia E.S.A. Distribution and degradation of terrestrial organic matter in the sediments of peat-draining rivers, Sarawak, Malaysian Borneo. *Biogeosciences* **2019**, 16 (22Spec.Iss.), 4517-4533.

APPENDIX A

Figures S1-S8

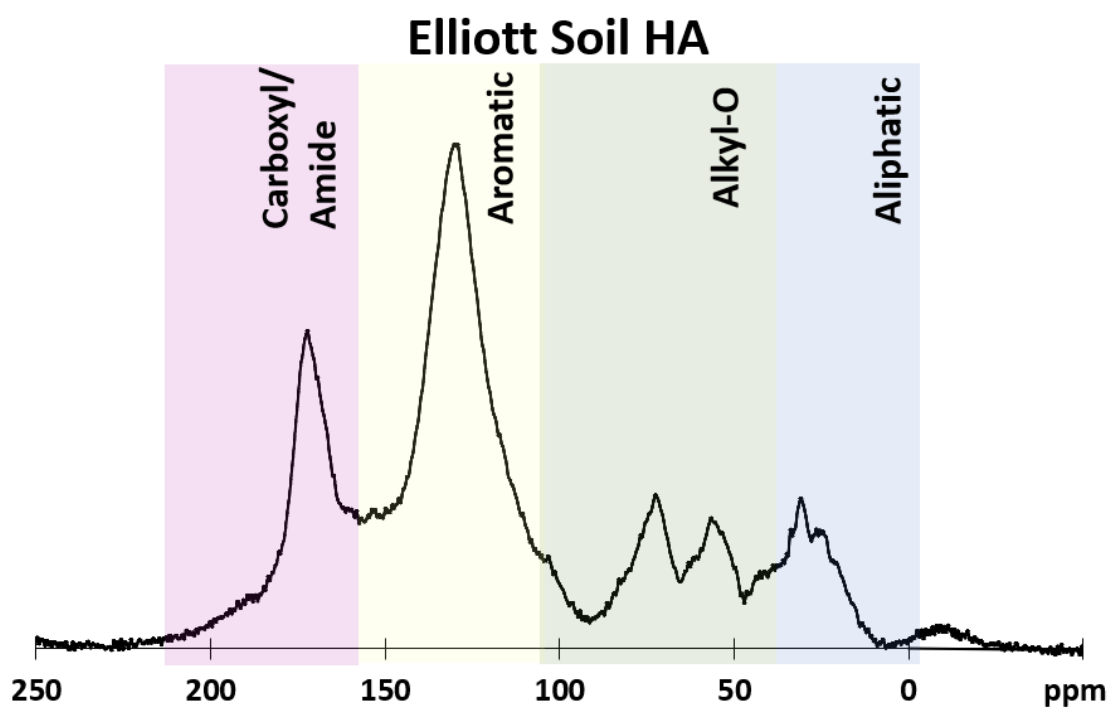


Fig. S1. Solid-state ^{13}C NMR spectrum of International Humic Substances Society (IHSS) Elliott soil humic acid extract. This sample was obtained from IHSS reference sample collection.

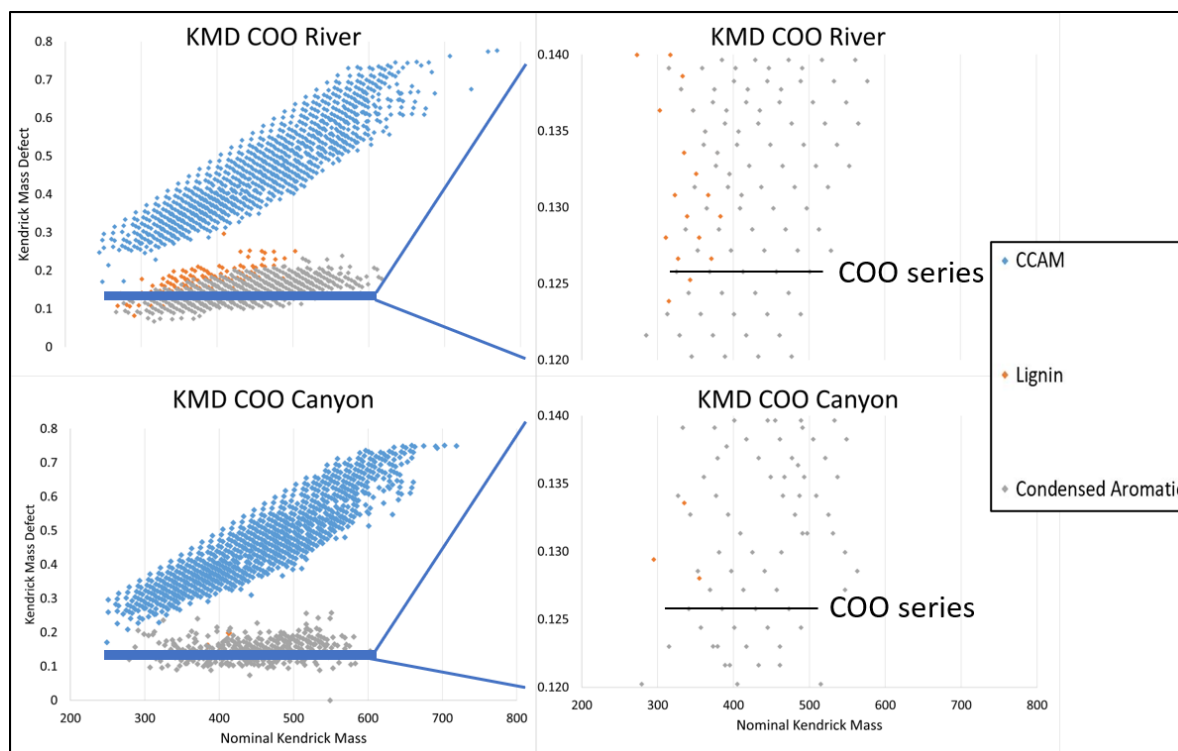


Fig. S2. KMD series for COO of the river and canyon. Right image is a zoomed in slice to better show the homologous series. The homologous series indicates a true formula (Sleighter and Hatcher, 2007). These true formulae are “likely” correctly assigned while others that do not fit this criterion can be eliminated as “not likely” correct assignments.

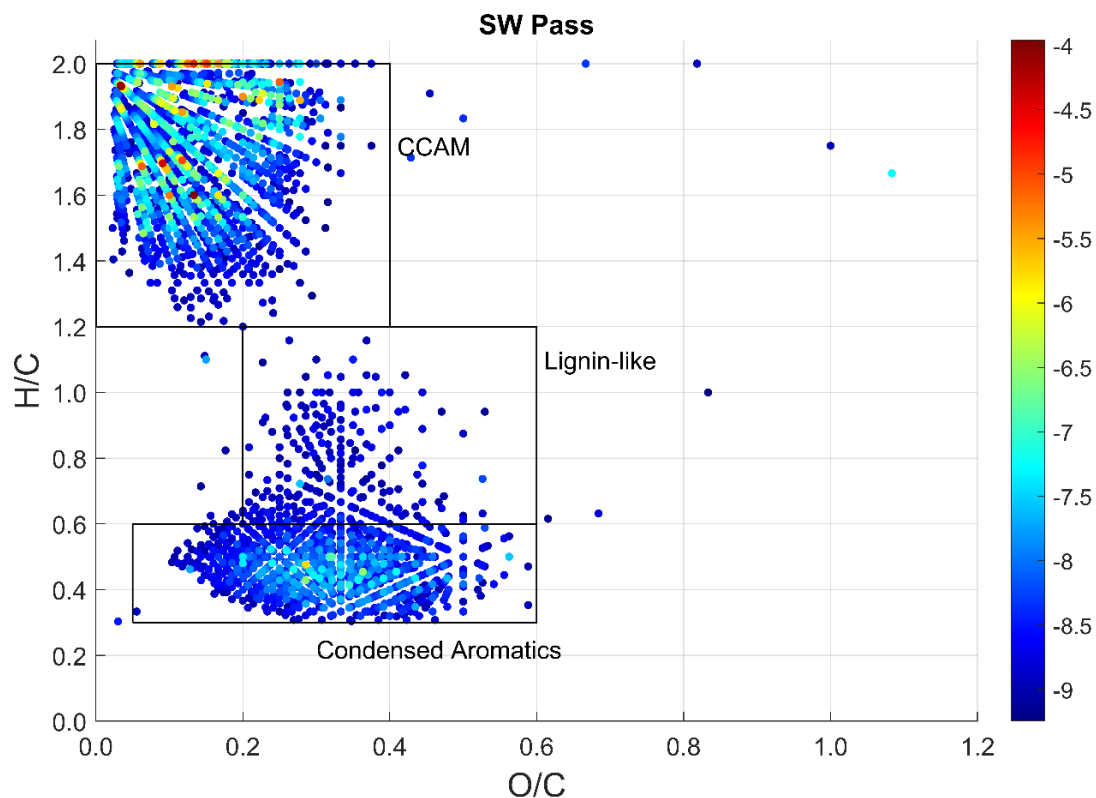


Fig. S3 Negative ion ESI-FTICR-MS data for humic acid extracts of the SW Pass. The van Krevelen plot includes a log scale of relative intensities. Includes focus boxes around the CCAM, Lignin-like, and Condensed Aromatics regions as described in section 3.3 above to aid in visualization between samples.

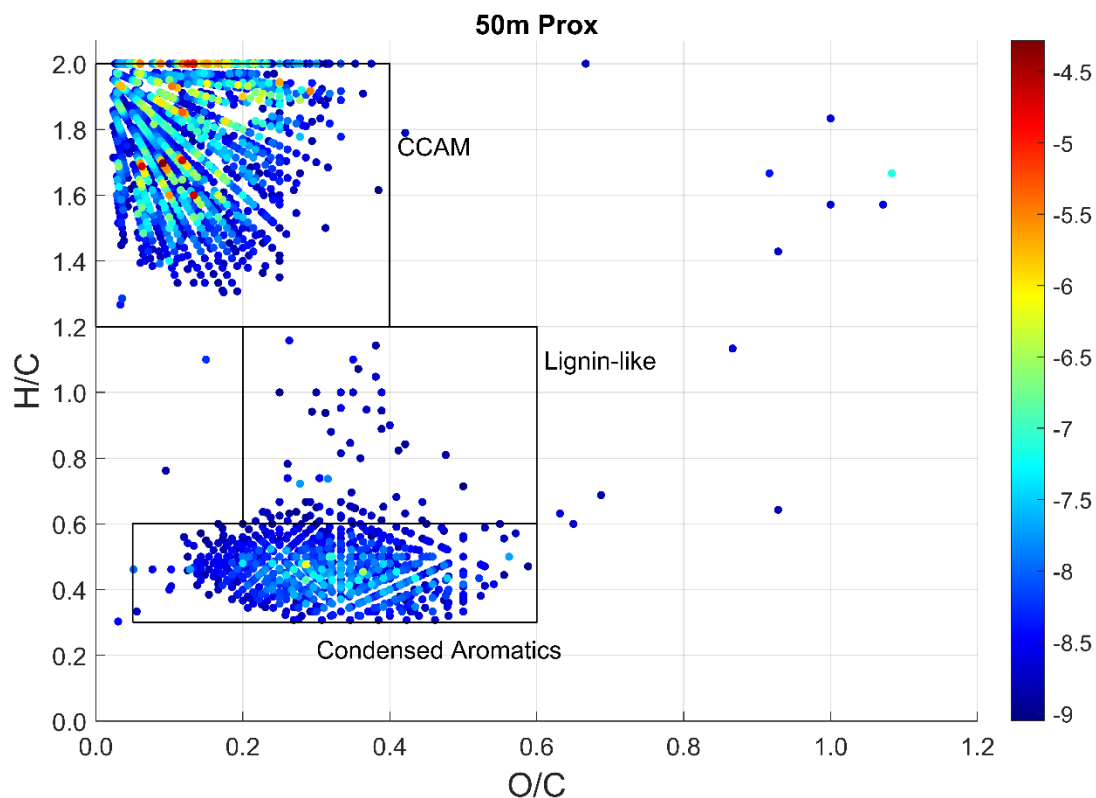


Fig. S4 Negative ion ESI-FTICR-MS data for humic acid extracts of the 50m Prox. The van Krevelen plot includes a log scale of relative intensities. Includes focus boxes around the CCAM, Lignin-like, and Condensed Aromatics regions as described in section 3.3 above to aid in visualization between samples.

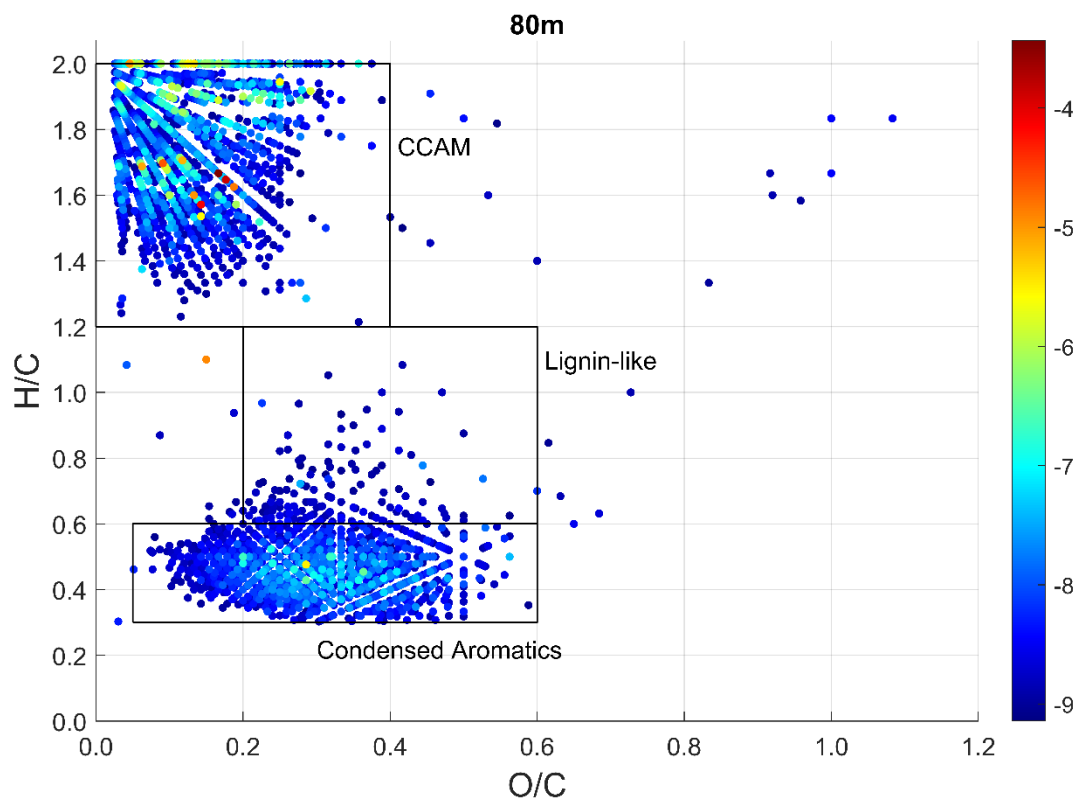


Fig. S5 Negative ion ESI-FTICR-MS data for humic acid extracts of the 80m. The van Krevelen plot includes a log scale of relative intensities. Includes focus boxes around the CCAM, Lignin-like, and Condensed Aromatics regions as described in section 3.3 above to aid in visualization between samples.

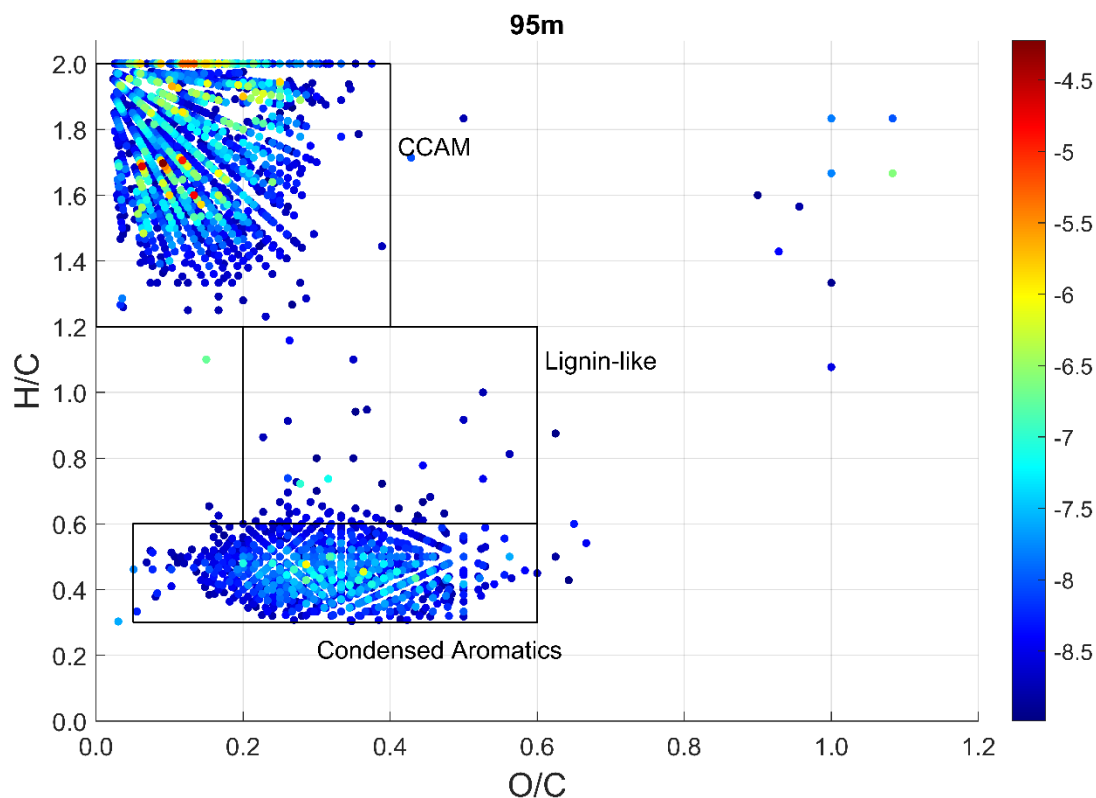


Fig. S6 Negative ion ESI-FTICR-MS data for humic acid extracts of the 95m. The van Krevelen plot includes a log scale of relative intensities. Includes focus boxes around the CCAM, Lignin-like, and Condensed Aromatics regions as described in section 3.3 above to aid in visualization between samples.

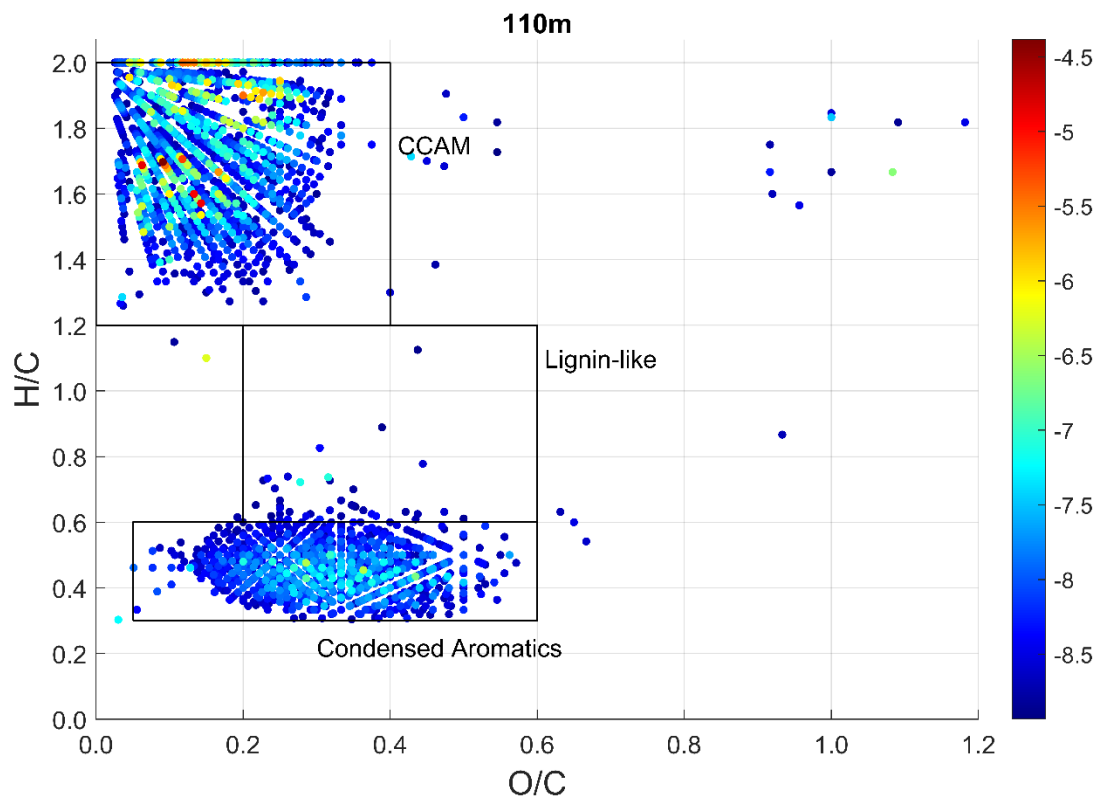


Fig. S7 Negative ion ESI-FTICR-MS data for humic acid extracts of the 110m. The van Krevelen plot includes a log scale of relative intensities. Includes focus boxes around the CCAM, Lignin-like, and Condensed Aromatics regions as described in section 3.3 above to aid in visualization between samples.

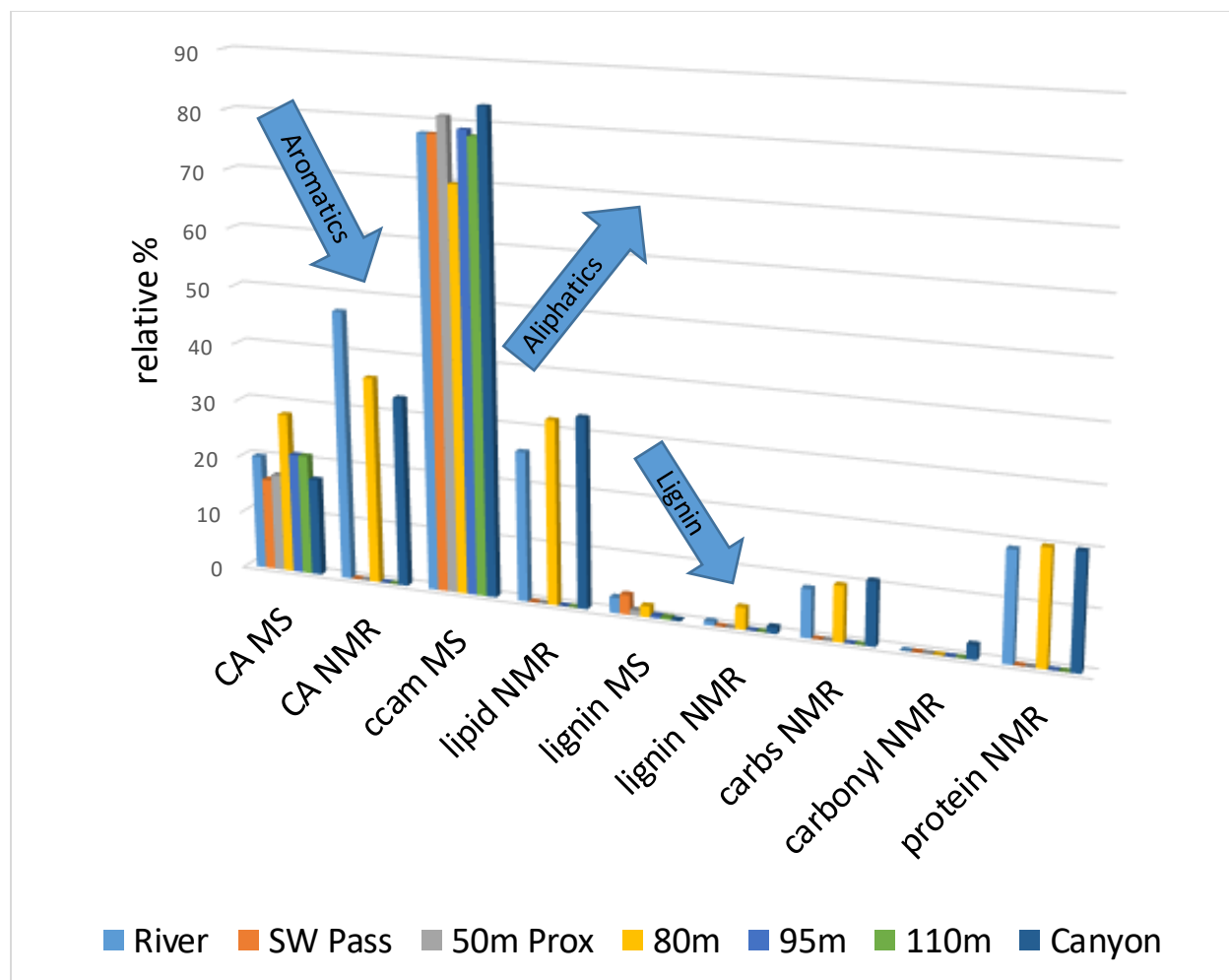


Fig. S8 Relative peak intensity percentages (r%) of molecular data for the HA extracts from FTICR-MS analysis (MS) and NMR peak data converted by the structural assignment software proposed by Baldock et al. (2004). Relative intensity from defined regions on the van Krevelen diagram MS data and relative intensity from NMR structural assignment software utilizing molecular mixing models, as proposed by Baldock et al. (2004)

APPENDIX B

Table S1

Table S1. Relative peak intensity percentages (r%) of molecular data for the HA extracts from FTICR-MS analysis (MS) and NMR peak data converted by the structural assignment software proposed by Baldock et al. (2004).

Sample	condensed aromatic MS (r%) ^a	condensed aromatic NMR (r%) ^b	ccam MS (r%) ^a	lipid NMR (r%) ^b	lignin MS (r%) ^a	lignin NMR (r%) ^b	carbo-hydrates NMR (r%) ^b	carbonyl NMR (r%) ^b	protein NMR (r%) ^b
River	20	47	78	26	2.7	0.65	8.4	0	19
SW Pass	16	<i>n/a</i>	78	<i>n/a</i>	3.4	<i>n/a</i>	<i>n/a</i>	<i>n/a</i>	<i>n/a</i>
50m Prox	17	<i>n/a</i>	81	<i>n/a</i>	0.91	<i>n/a</i>	<i>n/a</i>	<i>n/a</i>	<i>n/a</i>
80m	28	36	70	32	1.9	3.8	9.6	0	20
95m	21	<i>n/a</i>	79	<i>n/a</i>	0.40	<i>n/a</i>	<i>n/a</i>	<i>n/a</i>	<i>n/a</i>
110m	21	<i>n/a</i>	78	<i>n/a</i>	0.35	<i>n/a</i>	<i>n/a</i>	<i>n/a</i>	<i>n/a</i>
Canyon	17	33	83	33	0.15	1.1	11	2.5	20

^a relative intensity from defined regions on the van Krevelen diagram MS data

^b relative intensity from NMR structural assignment software utilizing molecular mixing models, as proposed by Baldock et al. (2004)

VITA

Sarah Ann Ware

4501 Elkhorn Ave Chemistry Buildingsware006@odu.edu
Norfolk, VA 23529

Education

May 2015B.S. Chemistry, Old Dominion University
Norfolk, Virginia

May 2023 (anticipated)M.S. Chemistry, Old Dominion University
Norfolk, Virginia

Presentations

1. “The Fate of Terrigenous Organic Matter Exported from the Mississippi River Delta to the Gulf of Mexico” Poster presentation at the 49th Annual Organic Geochemistry Gordon Research Conference, Holderness, NH, USA. July 29- August 3, 2018.
2. “The Fate of Terrigenous Organic Matter from the Mississippi River Delta to the Canyon of the Continental Shelf, Gulf of Mexico” Oral presentation at the 19th International Conference of International Humic Substances Society, Albena Resort, Bulgaria. September 16-21, 2018.
3. “The Fate of Terrigenous Organic Matter Exported from Major River Systems to Oceans” Departmental seminar at Old Dominion University, Norfolk, VA. November 2, 2018.

Publications

Ware, Sarah A., Hartman, Blaine E., Waggoner, Derek C., Vaughn, Derrick R., Bianchi, Thomas S., Hatcher Patrick G., (2022) Molecular evidence for the export of terrigenous organic matter to the north Gulf of Mexico by solid-state ¹³C NMR and Fourier transform ion cyclotron resonance mass spectrometry of humic acids, *Geochimica et Cosmochimica Acta*, Volume **317**, 2022, Pages 39-52, ISSN 0016-7037, <https://doi.org/10.1016/j.gca.2021.10.018>.

Awards:

Graduate Teaching Assistant of the Year - 2021